KME

CONSORTIUM MATERIALS TECHNOLOGY for demonstration and development of thermal energy processes

# Increased electrical efficiency and service life assessment of super heaters from combustion of difficult fuels


Fortum:
Thomas Svärd, Hans Larsson and Eva-Katrin Lindman

WSP:
Solvie Herstad Svärd

Chalmers:
Andrea Olivas, Erik Larsson, Dongmei Zhao, Torbjörn Jonsson and Jesper Liske


KME-514

# Increased electrical efficiency and service life assessment of super heaters from combustion of difficult fuels

Fortum:
Thomas Svärd, Hans Larsson and Eva-Katrin Lindman
WSP:
Solvie Herstad Svärd
Chalmers:
Andrea Olivas, Erik Larsson, Dongmei Zhao, Torbjörn Jonsson and Jesper Liske

KME-514

# Preface

The project has been performed within the framework the fifth stage of the material technology research programme KME.

KME, Consortium Materials technology for demonstration and development of thermal Energy processes, was established 1997 on the initiative of the Swedish Energy Agency. In the consortium, the Swedish Energy Agency, seven industrial companies and 18 energy companies participate. The programme stage has been financed with 60.2 % by participating industrial companies and with 39.8 % by Swedish Energy Agency. The consortium is managed by Elforsk.

The programme shall contribute to increasing knowledge to forward the development of thermal energy processes for various energy applications through improved expertise, refined methods and new tools. The programme shall through material technology and process technology developments contribute to making electricity production using thermal processes with renewable fuel more effective. This is achieved by

- Forward the industrial development of thermal processes through strengthen collaboration between industry, academy and institutes.
- Build new knowledge and strengthen existing knowledge base at academy and institutes
- Coordinate ongoing activities within academy, institutes and industry

KME's activities are characterized by long term industry relevant research and constitutes an important part of the effort to promote the development of new energy technology with the aim to create an economic, environmentally friendly and sustainable energy system.

# Abstract

In summary, the project has investigated how probe exposures and tube exposures correlate and how the corrosion rates change over time. This has been done at two positions at SH2 and at current superheater temperature as well as an increased temperature. In addition, the deposit formation has been coupled to the flue gas chemistry and fuel composition for short term exposures.

# Sammanfattning

Nyckelord: Sondförsök, korrosionshastighetsmätningar, korrosion i avfallspannor, koppling mellan bränslesammansättning och beläggning

Detta projekt har haft som mål att förbättra anläggningars ekonomi genom att ta fram grundläggande kunskap hur sondförsök kan användas för att estimera livslängden hos överhettare. Det är allmänt känt att sondförsök överdriver den verkliga korrosionshastigheten hos de överhettare som sondförsöken syftar till imitera. Målet att förbättra livslängdsbedömningar delas även med KME509 och genom att utföra likartade försök i de två projekten blir kunskapen mer generell. Den kunskap som uppkommit inom projektet är till nytta för flertalet aktörer inom kraftvärmebranschen så som pannägare, panntillverkare samt materialtillverkare.

Projektet har framgångsrikt genomfört en omfattande exponeringsmatris inkluderande 12 sondförsök samt 2 testsektioner i den befintliga överhettaren exponerade tidsupplöst upp till 3600 timmar. Av dessa 12 sondförsök har 6 varit av kortare karaktär (4 timmars exponeringar) vars främsta syfte har varit att följa beläggningens tillväxt och dess sammansättning. Vidare har tre olika material undersökts vid två olika materialtemperaturer vid två olika positioner i överhettaren, vilket gett korrosionshastigheter både vid befintlig materialtemperatur på dagens överhettare samt en temperatur som syftar till framtida pannor med höjda ångdata.

Resultaten från projektet visar att korrosionshastigheterna för de undersökta materialen (T22, 304L och 347H) vid den valda positionen (ÖH2) i pannan är överlag låga, vilket överensstämmer med korrosionshastigheten som uppmätts på de befintliga överhettarna, som hitintills har en livslängd på nästan 14 år. Även om korrosionshastigheten för de olika materialen har varit likartad så har korrosionsangreppet skilt sig åt. För 304L dominerades korrosionsattacken av lokala angrepp emedan övriga delar uppvisade gott korrosionsmotstånd. För T22 var attacken av mer allmän karaktär och det fanns inget område med tunn oxid. En del av förklaringen till de olika korrosionsangreppen föreslås bero på hur sonderna startas; proverna värms långsamt upp i en mild miljö vilket föroxiderar proven.

Projektet undersökte också om det fanns någon inneboende skillnad mellan korrosionshastigheten av sondexponerade prover och överhettare. Enligt resultaten, verkar det inte föreligga en sådan skillnad. Dock krävs det att sondförsöken i möjligaste mån efterliknar överhettarens termiska och miljömässiga historia. Speciellt fokus bör riktas på hur sondexponeringarna startas. Resultaten indikerar att en start med kalla sonder direkt in i en varm panna påverkar korrosionsangreppet negativt.

Sammanfattningsvis har vi inom projektet visat på hur korrosionshastigheter mellan sondexponerade och tubexponerade prov korrelerar samt hur dessa förändras med tiden. Detta genomförts vid två positioner i ÖH2, både vid befintlig temperatur och vid en temperatur som siktar på framtida pannor med höjda ångdata. Vidare har projektet undersökt hur bränslesammansättning, rökgaskemi samt beläggningsinnehåll förhåller sig till varandra. Slutsatsen från projektet är att sondexponeringar är ett möjligt sätt för att undersöka den potentiella korrosionshastigheten av överhettare.

# Summary

Keywords: probe exposures, corrosion rate determination, corrosion in waste fired boilers, Correlation between fuel and deposit composition

The main aim of this project has been to improve the plant economy by generating fundamental knowledge about how probe exposures can be used in order to estimate the lifetime of the superheater. The corrosion rate obtained from the probe exposures usually exaggerates the actual corrosion rate of the superheaters. This aim has also been addressed by KME509 and by performing similar exposures in two boilers the results will be more general in character. The knowledge generated within the project is beneficial to several actors within the power industry, e.g. boiler owners, boiler manufacturers and materials producers.

The project has successfully executed a comprehensive exposure matrix including 12 probe exposures and 2 test sections in the existing superheater exposed in time resolved manner up to 3600 hours. Of the 12 probe exposures, 6 were of short term character (i.e. 4 hours) investigating the deposit formation. The exposure matrix included 3 materials and 2 material temperatures, performed at two positions in the superheater bundle. The two temperatures were chosen so that corrosion issues at current as well as future steam temperatures were investigated.

The results show that corrosion rates of the exposed probe samples (T22, 304L and 347H) are generally low, which is consistent with the corrosion rate measured at the existing superheater 2 bundle (the current lifetime is nearly 14 years). Even though the corrosion rate was similar, the corrosion morphology of the T22 and 304L samples were different. In the case of 304L, the corrosion attack was localized whereas for T22 the attack was of more general nature. It is suggested that this is due to the start-up sequence of the probes; being pre-oxidized in a mild environment during boiler start after revision.

The project also investigated if there was any inherent difference between the corrosion rate of probe exposed samples and the superheaters. According to the results, it does not seem to exist such a difference. Hence, probe exposures are a possible way of investigating the potential corrosion rate of superheaters. However, it is important to stress that the probe exposures needs to, as far as possible, mimic the thermal and environmental history of the superheater. The results indicate that a startup with cold probes directly into a hot boiler affect corrosion attack negatively.

In summary, the project has investigated how probe exposures and tube exposures correlate and how the corrosion rates change over time. This has been done at two positions at SH2 and at current superheater temperature as well as an increased temperature. In addition, the deposit formation has been coupled to the flue gas chemistry and fuel composition for short term exposures. The conclusion from the project is that probe exposures are a relevant for estimating the life time of superheaters.

# Table of contents


**1 Introduction 1**

1.1 Background 1
1.2 Description of the research field 2
1.3 Research task 2
1.4 Goal 3
1.5 Project organization 3

**2 Plant description 5**

2.1 Boiler P6 5
2.2 The waste fuel 8

**3 Experimental conditions 9**

3.1 Operating data during October 2012 - March 2013 9
3.2 Probe and tube exposures 13
3.2.1 Materials 13
3.2.2 Probes location and description 13
3.2.2.1 Position 1 14
3.2.2.2 Position 2 15
3.2.3 Evaluation of probe and tube samples 16

**4 Results 19**

4.1 Short-term probe exposures 19
4.2 Long-term exposures 26

**5 Analysis of the results 39**

**6 Conclusions 43**

**7 Goal fulfilment 44**

**8 Suggestions for future research work 45**

**9 Literature references 46**

**10 Publications 48**

# 1 Introduction

## 1.1 Background

Renewable energy sources such as biomass and waste are important for the Swedish energy supply. However, these fuels are challenging to combust because of their heterogeneous nature and the relatively high levels of alkali and chlorine. The fuel composition results in a flue gas environment that is more corrosive compared to fossil fuels. Actually, fireside corrosion is the main lifetime limiting factor for the superheaters in these plants and puts an upper limit to the steam data. In addition, the high ash content results in the formation of deposits on heat-exchanging surfaces (fouling) that limits power production.

Much research has been directed towards fireside corrosion and fouling in these plants in order to decrease maintenance costs and enable increased power efficiency. The in-plant work has mostly used cooled probes in order to investigate e.g. the influence of fuel composition, fuel additives, material composition and material temperature on fireside corrosion. The work has resulted in great improvement of the level of knowledge, e.g. concerning the influence of fuel composition and certain fuel additives on the rate of fireside corrosion. Much remains to be done however, for example concerning predicting the service life of superheaters.

The background for this project is derived from the usually poor estimations on corrosion rate of the superheaters in biomass and waste fired boilers. Hence, this current project shares the same background as the KME 509 project, performed at the P14 boiler at Händelöverken. By performing this type of extensive exposure matrix in two different boilers, the aim have been to get a more general understanding about how probe exposures can be performed in order to obtain quantitative corrosion rates applicable for estimations of the service life of the installed superheater. Especially the discrepancy between probe and tube exposed samples have been addressed. Compared to KME 509, a more detailed analysis of the deposit formation have been performed in a time resolved manner. Better estimations of the superheater corrosion will lead to better plant economy as changing a superheater is usually associated with great costs. Today, the estimated corrosion rate of the superheaters is usually extrapolated from probe measurements, exposed for a certain time (e.g. 1000 hours). Due to the limitations of these estimations, the boiler owners are instead planning upcoming changes of the superheaters by performing thickness measurements of the superheater bundle during the yearly revision.

In addition to increasing the knowledge about quantitative corrosion testing, this project has also performed an extensive matrix of short term deposit testing. By this frequent probe testing and large effort in analysis, the variations in fuel composition have been coupled to the flue gas chemistry and deposit composition, over a period of 6 months. Furthermore, this project has been performed in parallel to a project investigating how the fouling (i.e.

deposit build-up) of the boiler is progressing with time. By increasing the knowledge about how the fuel, gas chemistry and deposit composition is connected, the model for fouling may be improved. Hence, this project can be separated in two main parts.

## 1.2 Description of the research field

It is known that the fireside corrosion rates measured in cooled probe exposures are usually higher (sometimes much higher) compared to corrosion rates of tubes in real superheater bundles. The causes behind this discrepancy are largely not understood and have not been subjected to systematic study. This is a huge drawback limiting the usefulness of cooled probe exposures for predicting superheater lifetime. One central aim of this work is to address this problem and to analyse different parameters that may explain this discrepancy. Within this type of corrosive environments, i.e. biomass or waste combustion, there have been a great number of tests throughout the years where probe testing directed towards quantitative corrosion rate measurements has been performed [1-18].

In order to achieve as realistic corrosion rate values as possible, with respect to comparing the corrosion rates of the probes as with the corrosion rate of the superheaters, some issues needs to be addressed. One crucial factor is that while cooled probe corrosion exposures are seldom longer than 1000 hours, the lifetime of the superheater is several years. Thus, the corrosion rate is linearly extrapolated from the corrosion rate during the first 1000 hours of exposure. Another factor that may be of importance of the overall corrosion rate is the start-up sequence. For superheaters, the start-up is slow, following the boiler start-up sequence, and the environment is non-corrosive (usually oil is used as fuel). In contrast, probes are usually started directly into the hot boiler, directly exposed towards the corrosive environment.

Because these factors are not known, it is necessary to study corrosion kinetics in order to better extrapolate the cooled probe data for lifetime prediction. The present project therefore involves time-resolved cooled probe exposures at different temperatures as well as tangent test sections of the superheater.

## 1.3 Research task

The background for this project is derived from the usually poor estimations on corrosion rate of the superheaters in biomass and waste fired boilers. Hence, this project shares the same background as the KME509 project, performed in the P14 boiler at Händelöverken. By performing this type of extensive exposure matrix in two different boilers, the aim has been to get a more general understanding about how probe exposures can be performed in order to obtain quantitative corrosion rates applicable for estimations of the service life of the installed superheater. Furthermore, the project focuses on understanding the discrepancy between corrosion rate measurements using cooled probes and the corrosion rate of the real superheater. This is done by comparing time resolved probe exposed samples with test sections installed in the superheater bundle.

In addition to corrosion testing, this project aims for correlating fuel composition, flue gas chemistry and deposit buildup. This is done by performing 6 deposit probe exposures over a 6 month period. Special emphasis is put on the deposit growth and deposit chemistry linked to the boiler performance and fuel composition. These issues have been addressed in collaboration with a parallel project at Högdalen (the fouling project performed by Fortum and WSP) where a model for fouling based on measuring the heat transfer is under development. This model uses logged data from the P6 boiler and calculates the fouling tendency (as a factor) of chosen parts of the heat transfer surfaces, including the empty shaft, SH1, SH2 and the economizer.

In order to fulfil these tasks, a comprehensive exposure matrix consisting of both tube and probe exposed samples have been carried out. The matrix consisted of time resolved probe exposures (24, 1000, 2000 and 3600 hours) and 2 test sections installed in the superheater bundle (exposed for 3600 hours).

## 1.4 Goal

The overall goal of the project is to improve plant economy by enabling an increased electricity production and enhancing fuel flexibility. This will be achieved by generating new knowledge to facilitate the development of models for determination of the service life of superheater materials as a function of material temperature. The project does also aim for increasing the understanding of deposit build-up and fouling. The project addresses the KME goal to verify an increase of the steam temperature by at least 50°C from 450 to 500°C for waste fractions. This is performed by increased material temperatures of a selection of the samples exposed by probes. The project focuses on understanding the discrepancy between corrosion rate measurements using cooled probes and the corrosion rate of the real superheater. This is done by comparing time resolved cooled probe corrosion rate measurements with exposures of sample materials installed in the superheater bundle.

## 1.5 Project organization

The project is jointly performed by Fortum and HTC at Chalmers. The distribution of work was:

| Part | Participants role in the project |
|---|---|
| Fortum Värme | Responsible for operation, gas and fuel analysis. Responsible for probes during operation. Coordinating the work of WSP. |
| Chalmers/HTC | Project management. Providing probes and sample materials for probes and tubes. Responsible for probe and tube mantling and dismantling. Responsible for corrosion evaluation and service life assessment. |

**Table 1. Participating partners in the KME-514 project.**

The members of the reference group were, besides members of the project;

| | |
|---|---|
| Anna Jonasson | Eon Värme Sverige |
| Bo Jönsson | Sandik Heating Technology |
| Hans Sundbeck | Metso Power |
| Pamela Henderson | Vattenfall Research & Development |

The project was financed within the frame work of KME by the Swedish Energy Agency. The total project budget was 2 511 kSEK.

This project has been performed in collaboration with the Fouling project, managed by WSP. The Fouling project uses a special program “PANYL-drift” in order to assess the degree of fouling of the different heat transfer surfaces in boiler. The program calculates so called fouling factors for different parts of the boiler. The fouling factors are related to a reference point when the boiler is clean and should only be compared relatively this reference point. Relative comparisons of the fouling factors can be used with good results in both long and short-term evaluations.

# 2 Plant description

Högdalen Heat and Power station 7 km south of Stockholm city is owned and operated by Fortum Värme. The Heat and Power station has five boilers for combustion of different waste fuels. In boiler 1-4 household waste is incinerated. The boiler 6 utilizes sorted and recycled waste mainly paper, wood and plastic from the society and industry. The P6 waste input is about 190 000 ton per year and the energy production about 550 GWh, electricity and heat.

The P6 plant consist of fuel handling system, boiler, a common steam turbine, a dry flue gas cleaning and flue gas condensing system.

**Figur 1. Bild över panna P6 vid Högdalenverket**

***Figure 1. Image of boiler P6 at Högdalenverket.***

## 2.1 Boiler P6

Boiler P6 at Högdalenverket is a compact 91.2 MWth CFB built by Foster Wheeler. The plant was commissioned 1999. The heat transfer surfaces in the boiler back pass consist of super heaters 1, 2 and an economizer. The hottest superheaters “Intrex” 3a and 3 b are placed in the return leg and are not evaluated in this project. The generated steam has a pressure of approximately 60 bar and a temperature of 480 °C. A schematic view of the boiler P6 is seen in Figure 2.

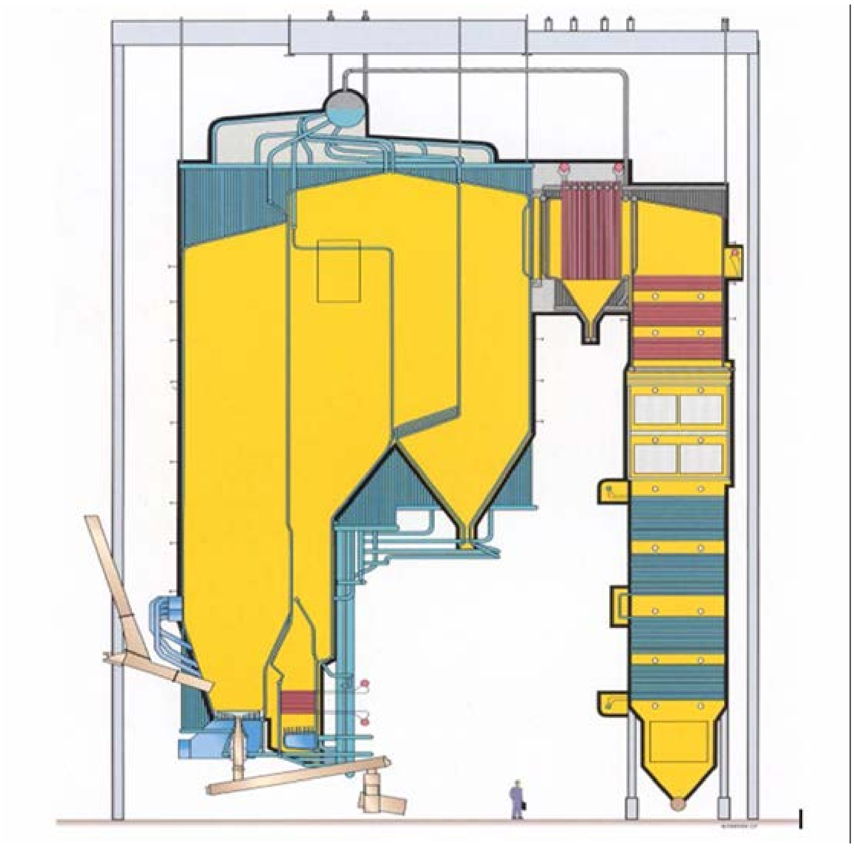

**Figur 2. Skiss av panna P6 vid Högdalenverket**

***Figure 2. The layout of boiler P6 at Högdalenverket.***

The major difference between a compact CFB and a traditional CFB boiler is that the cyclone is integrated with the furnace instead of being a standalone unit. This means that the cost of materials during construction is significantly less. The compact design does however lead to a less effective separation of coarse particles compared to stand alone cyclones. To improve the performance of the separation, the corners inside the cyclone are rounded.

Boiler P6 has three fuel lines, each having three separate fuel silos and the fuel is fed at the bottom of the furnace. The fuel is fluidized together with the bed material by means of the primary air fan. The secondary air fan supplies the furnace with additional combustion air and creates a mixing of the fuel and air in order to achieve an optimal combustion. The inlets of the secondary air are divided into two regions, one lower and one upper. The boiler is designed in a way so that the majority of the combustion occurs in the lower region and therefore the main part of the air is directed there.

The flue gases is led to the separators where the majority of the solid particles are separated and entering to two loop seals in which two particle super heaters – also called INTREX super heaters (SH3a and SH3b) are located. These super heaters are completely embedded in the sand bed, which decreases the effect of the corrosive environment. In order to avoid problems related to erosion it is important that the sand bed reaches sufficiently high in order to protect the tubes. INTREX – super heaters is the final superheating for process steam and by taking advantage of the extra heat from the sand, one can achieve a better steam data. The sand is returned to the sand bed in the furnace after the loop seal.

Boiler P6 system for bottom ash removal consists of three separate outputs from the bottom of the furnace and led to three water cooled chain conveyors. These lead to a joint chain conveyor that has been fitted with a coarse sieve in order to separate out large particles. The finer fractions continue through the coarse and through a drum sieve where only the finest fractions come through and taken to the sand transmitter which is a pressurized vessel and returned by the bed particles to the boiler. There is also ash removal from the empty pass and at SH2. However, no ash from these positions is returned to the boiler.

The flue gases continues after the separator through two center tubes down to an empty pass where additional cooling is occurring by water cooled walls. After the empty pass two super heaters (SH1 and SH2) are located. After SH1 and SH2 the flue gases passes through the economizer before going to the flue gas cleaning.

The boiler has extensive sootblowing consisting of water soot blowing of the empty shafts, steam sootblowing of the boiler screen and superheater 2, hammers on superheater 2 and rotating full-length steam sootblowing in superheater 1 and 2. The economizer has a sonic sootblower, but its effect has been questioned. Details regarding the sootblower systems are found in Table 2.

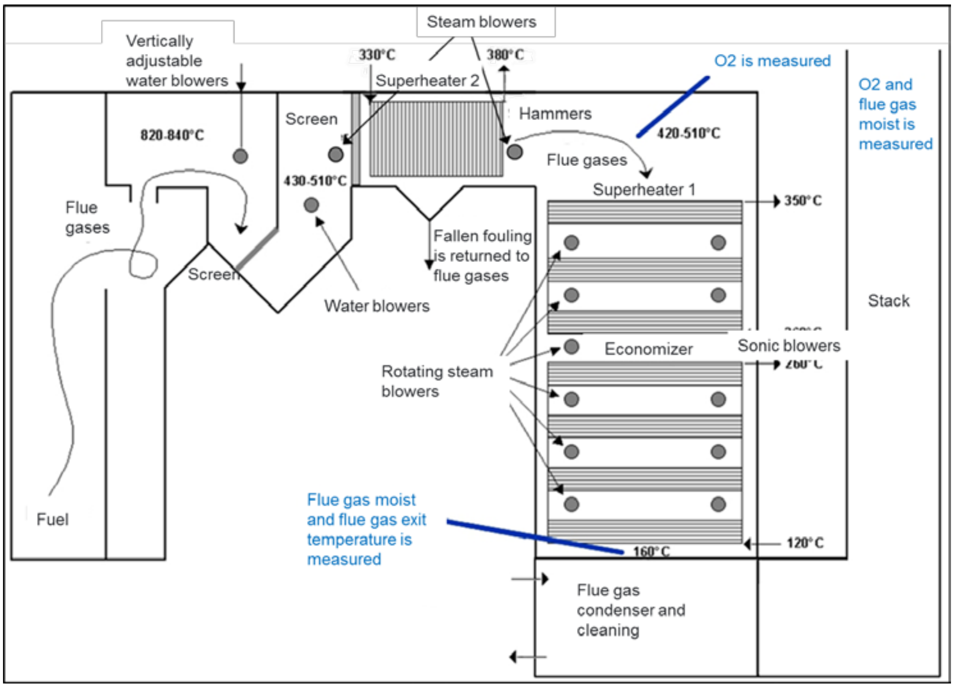


**Figur 3. Schematisk bild över värmeväxlarsystemet vid panna P6 vid Högdalenverket**

***Figure 3. Schematic view of the heat recovery system and sootblowing in boiler P6 at Högdalen Heat and Power station***

| **Surface** | **Sootblower** | **Frequency** |
|---|---|---|
| Empty shafts, hanging smooth tubes | Water sootblower | 1 time/day |
| Boiler screen | Steam sootblower | 3 times/day |
| SH 2, hanging smooth tubes | Steam sootblower | 3 times/day |
| -„- | Hammers | 3 times/day |
| SH 1, horizontal smooth tubes | Steam sootblower | 3 times/day |
| Economizer, horizontal smooth tubes | Steam sootblower | 3 times/day |
| -„- | Sonic sootblower | 1 time/min 5 s |

**Table 2. Sootblowing equipment of boiler P6 in Högdalen (2011)**

## 2.2 The waste fuel

The main fuel used in the boiler is PTP, paper, wood and plastics, which have relatively high concentration of chlorine, which may cause deposits and corrosion, see Table 3. The complete fuel analyses are shown in appendix B.

| | **Mean values 2012 - 2013**[1] |
|---|---|
| *Moisture (weight-%)* | *28.3* |
| Ash *(weight-% d*s) | *17.2* |
| Coal *(weight-% d*s) | *45.2* |
| Hydrogen *(weight-% d*s) | *5.8* |
| Nitrogen *(weight-% d*s) | *0.8* |
| Sulphur *(weight-% d*s) | *0.6* |
| Chlorine *(weight-% d*s) | *0.4* |
| Oxygen *(weight-% d*s diff) | *29.9* |
| Calorific heating value (MJ/kg ds) | *18,7* |
| Lower heating value (MJ/kg ds) | *18,3* |

**Table 3. Fuel analysis boiler P6**

[1] From: Lindman 2013-03-18, ”Bränsleanalyse P6 KME Projektet”

# 3 Experimental conditions

## 3.1 Operating data during October 2012 - March 2013

The boiler P6 started up in October 2012 and data was collected from the 1st of October 2012 to the 10th of March 2013. Boiler load variation and highlighted incidents with large impact are found in Figure 4.

During the operating period, there were recurring problems with the fuel handling. For example, there have been problems with the output from the day silos. In the start-up period after the summer revision, the boiler had problems with the loop seal.

In the middle of December 2012, the boiler ran on part load due to problems with the fuel feeding. From the end of December 2012 to the beginning of January 2013, the boiler ran on part load due to clogging of the economizer. The boiler was shut down in the beginning of January 2013 due to a tube leakage and clogged bag filter. The stop continued for approximately 5 days during which the economizer was cleaned.

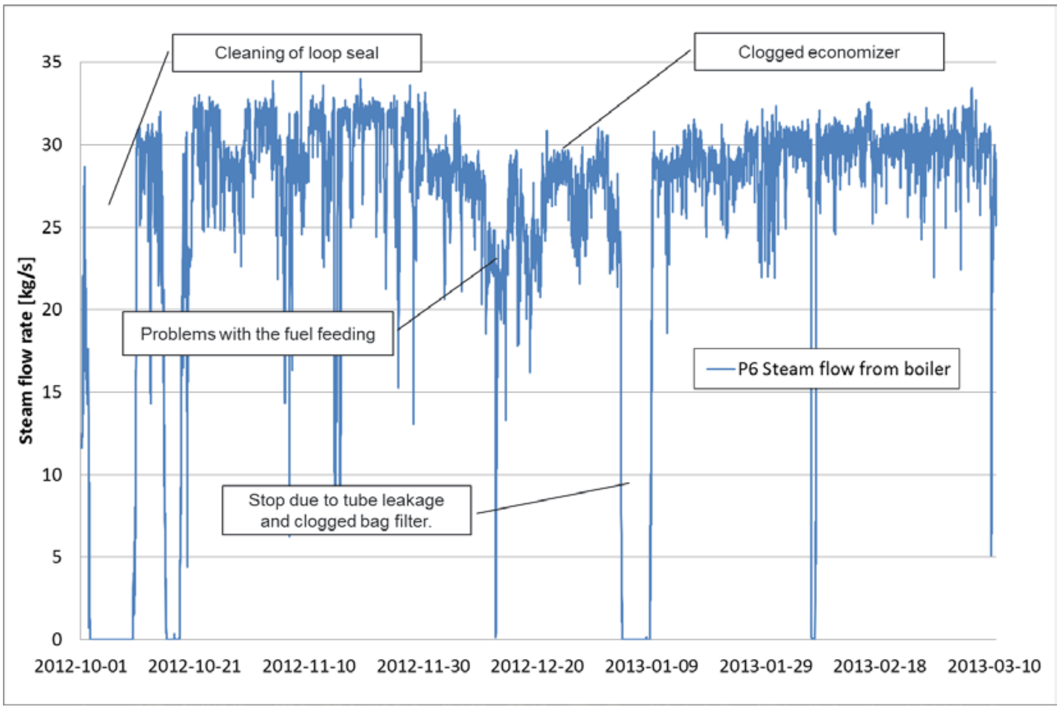


**Figur 4. Variationer i pannlast, oktober 2012 – mars 2013**

***Figure 4. Boiler load variation from October 2012 to March 2013.***

The $O_2$-levels after the furnace and in the stack (dry gas) are plotted in Figure 5.

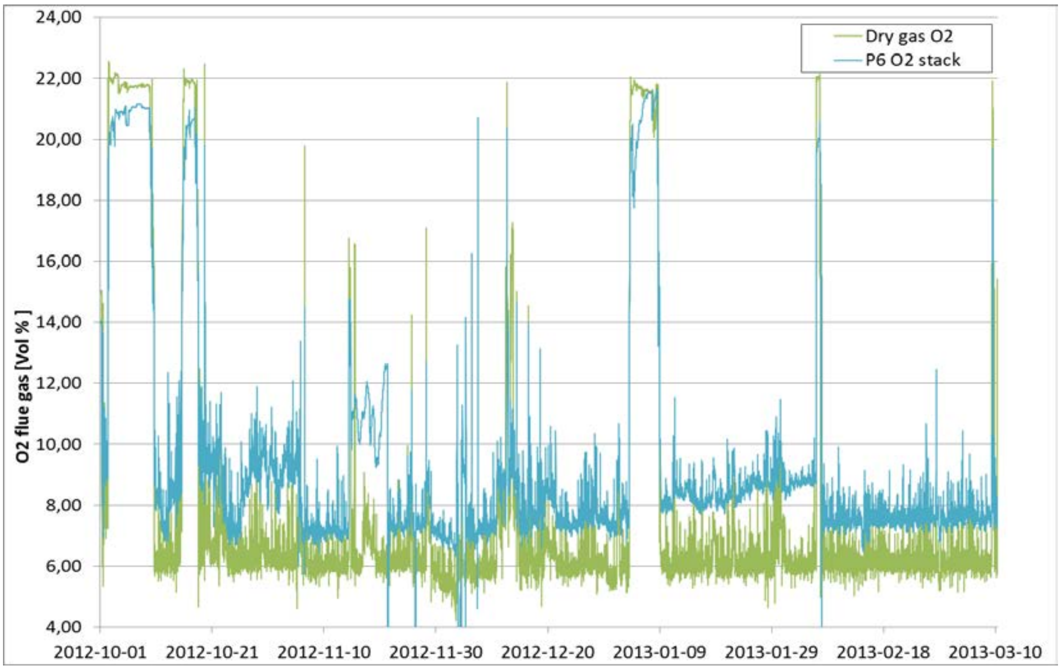


**Figur 5. $O_2$ nivåer i stack och panngas (torr gas) – oktober 2012- mars 2013**

***Figure 5. $O_2$ level in stack and furnace (dry gas) - October 2012 to March 2013.***

The $SO_2$ and HCl-levels are shown in Figure 6 and the steam flow and steam temperatures before and after the superheater 2 are shown in Figure 7. The results show a variation in both $SO_2$ and HCl over time. Interesting to note is the increase in $SO_2$ in the end of the period.

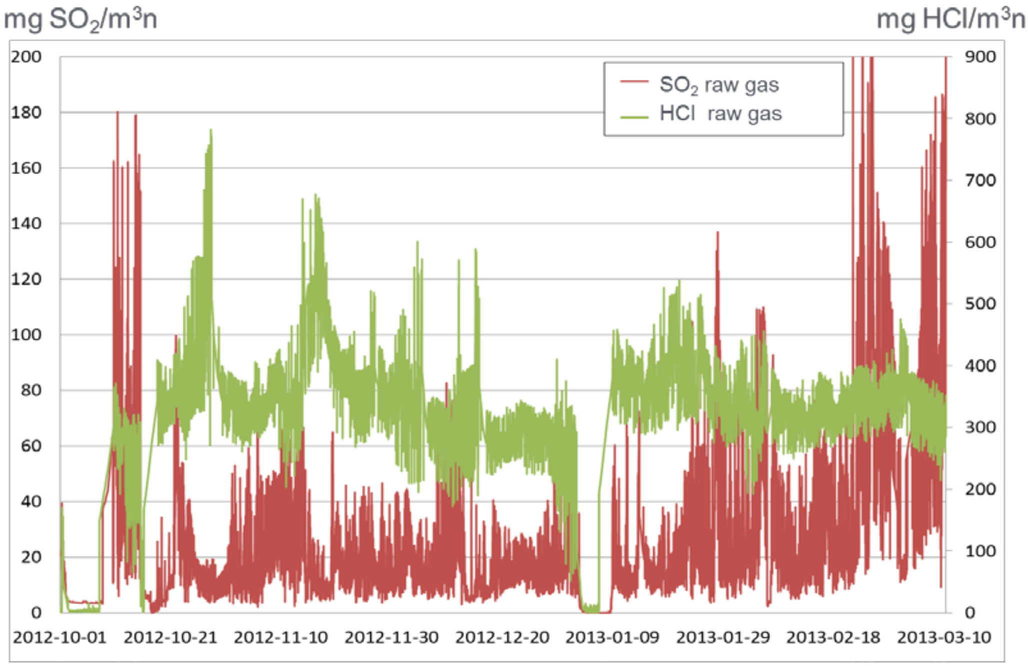


**Figur 6.** **$SO_2$ och HCl nivåer i rågas innan rökgasrening (mg/m³n dg@11% $O_2$)**

***Figure 6.*** ***$SO_2$ and HCl in raw gas prior to flue gas cleaning [ mg/m³n dg@11 % $O_2$]***

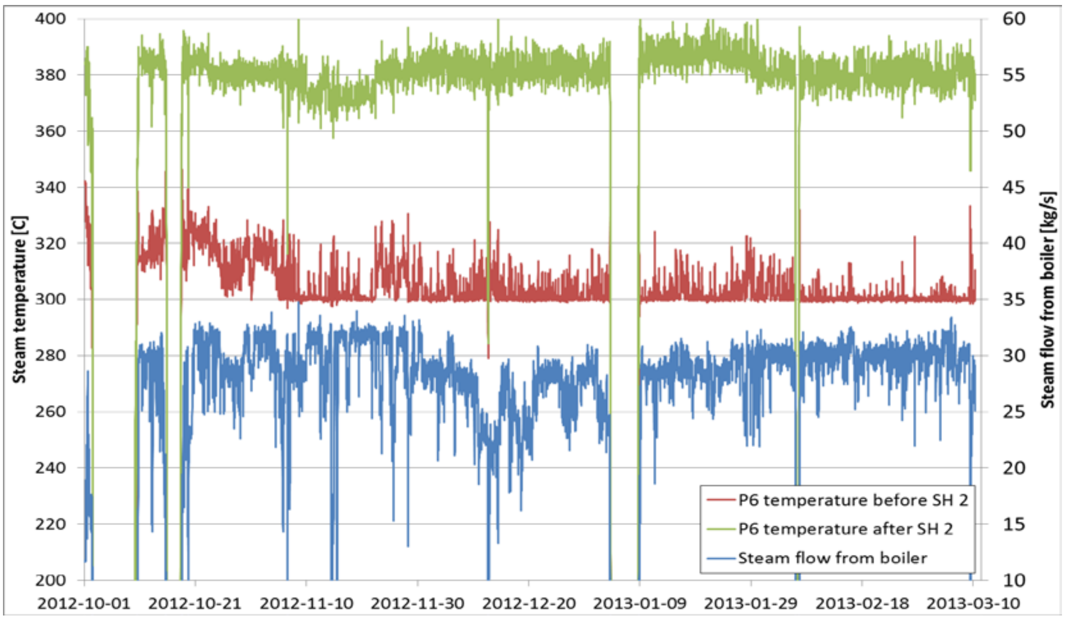


**Figur 7.** **Ångtemperaturer före och efter överhettare2 samt flödet av ånga, oktober 2012 – mars 2013.**

***Figure 7. Steam temperatures before and after superheater 2 and the steam flow from the boiler for the period October 2012 to March 2013.***

A summary of operating conditions during the 4 hour tests in P6 is found in Table 4.

| Date | | 2012-10-12 08:45-12:45 | 2012-10-29 10:25-14:25 | 2012-11-20 10:30-14:30 | 2013-01-02 11:20-15:20 | 2013-02-07 10:20-14:20 | 2013-03-08 10:13-14:13 |
|---|---|---|---|---|---|---|---|
| Load | kg steam /s | 29.9 | 28.8 | 32.1 | 25.0 | 28.9 | 29.5 |
| | MW | 91.0 | 89.8 | 91.1 | 80.2 | 86.6 | 89.5 |
| Furnace temperature (T) | 3,3 m | 858.0 | 808.5 | 840.7 | 825.8 | 853.4 | 852.6 |
| | 11 m | 855.8 | 855.6 | 896.7 | 881.1 | 897.9 | 854.4 |
| | 15 m | 839.4 | 839.8 | 876.6 | 873.9 | 878.4 | 855.1 |
| Flue gas temperature (T) | After second empty shaft | 520.2 | 515.7 | 542.9 | 530.2 | 553.2 | 559.8 |
| | After second empty shaft (calc.) | 593.0 | 583.0 | 641.0 | 625.8 | 635.2 | 662.8 |
| | After superheater no. 1 | 418.5 | 414.5 | 423.7 | 421.4 | 432.0 | 444.6 |
| | Before superheater no. 2 | 520.2 | 515.7 | 542.9 | 530.2 | 553.2 | 559.8 |
| | After superheater no. 2 | 454.1 | 454.8 | 464.5 | 463.4 | 473.7 | 484.5 |
| Steam temperature (T) | Before superheater no. 2 | 315.1 | 312.2 | 300.5 | 300.2 | 301.5 | 300.2 |
| | After superheater no. 2 | 385.0 | 379.9 | 370.7 | 382.1 | 376.2 | 379.8 |
| | Sat. temperature after drum | 281.8 | 281.2 | 282.6 | 278.9 | 281.3 | 281.3 |
| HCl | $mg/Nm^3$ dg 11 % $O_2$ | 196.6 | 418.5 | 280.8 | 286.3 | 264.4 | 224.1 |
| $SO_2$ | $mg/Nm^3$ dg 11 % $O_2$ | 28.7 | 3.8 | 12.3 | 7.2 | 185.5 | 50.0 |
| CO | ppm | 2.9 | 19.6 | 3.6 | 19.0 | 10.0 | 4.9 |
| $NO_x$ | $mg/Nm^3$ dg 11 % $O_2$ | 32.8 | 39.0 | 25.2 | 38.2 | 30.3 | 21.4 |
| $O_2$ | Furnace vol % dg | 6.1 | 6.4 | 6.1 | 6.2 | 6.2 | 6.1 |

**Table 4. Summary of operational conditions during the 4-hour probe tests.**

## 3.2 Probe and tube exposures

This project has been performed in parallel with KME509 and as far as possible the projects have shared the same experimental setup. However, due to practical issues and specific requests by the project members, there are experimental differences. The experimental parameters relevant for this project are addressed below.

### 3.2.1 Materials

The materials used for the short-term exposures were 304L and T22 and for the long-term exposures 304L, T22 and 347H. The chemical compositions are given in Table 5.

| Material | DIN/EN | Fe | Cr | Ni | Mn | Si | Mo | Nb | C | Others |
|---|---|---|---|---|---|---|---|---|---|---|
| 304L | 1.4306 | 68 | 19 | 10 | 1,4 | 0,6 | 0,5 | 0,08 | 0,03 | |
| AISI347H | 1.4550 | 68 | 17 | 11 | 1,7 | 0,6 | 0,3 | | 0,08 | Nb |
| T22 | 1.7380 | 96 | 2 | | 0,5 | | 1 | | 0,12 | |

**Table 5. Chemical composition (weight %) of tested materials.**

The alloys can be described as:

- 304L is a standard austenitic stainless steel alloyed with Cr and Ni. It has been used as water wall compound tubes in mainly Black Liquor Recovery Boilers. This is the low cost alternative both as austenitic stainless steel and compound tubes.
- 347H is a stainless steel stabilized with Nb for improved properties at high temperature.
- T22 (often referred to 10CrMo910) is a commonly used Cr-Mo-alloy low alloy steel in super heaters. It has good creep strength.

### 3.2.2 Probes location and description

The exposures were performed in superheater 2 at 2 different positions. Position 1 was placed before super heater. Most of the exposures were performed in this position. Position 2 was placed after the superheater. In this position, 2 long-term exposures were performed. Inside the superheater, material tubes were placed close to position 1 and 2. In the following figure (Figure 8) a schematic sketch of the probes location is shown.

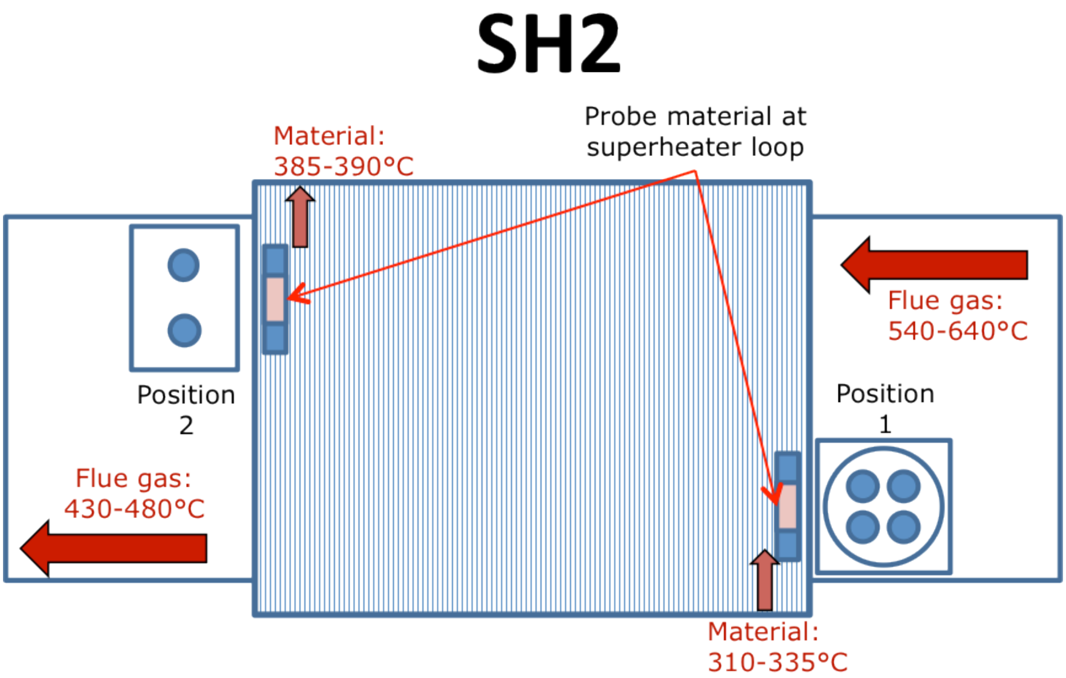


**Figur 8. Skiss över placering av sonder och tubprov vid ÖH2**

***Figure 8. Schematic sketch of probes and tubes at SH2.***

### 3.2.2.1 Position 1

In this study most of the exposures took place at this position. The position is located before the superheater 2. The man hole of position 1 consisted in 4 openings to place the probes into the superheater. At opening 1, 2 and 4, exposures of 1000, 3600 and 2000 hours were performed respectively. See Figure 9. Exposure of 24 hours was performed at opening 3. Once the exposure was finished, the opening 3 was used for 4 hours exposures.

Isothermal probes were built up for the exposures at this position. The temperature was measured with thermoelements located in line and directed against the flue gas. The probes were cooled with pressurizing air. On each probe 8 rings were placed in 2 zones. Each zone had different temperature, 455°C and 304°C. In Figure 9 is shown a schematic sketch of the used probe for this study.

The material tubes inside the super heater were placed close to the cooled probes. The materials tubes consisted in a 347H tube welded in both endings to T22 tubes.

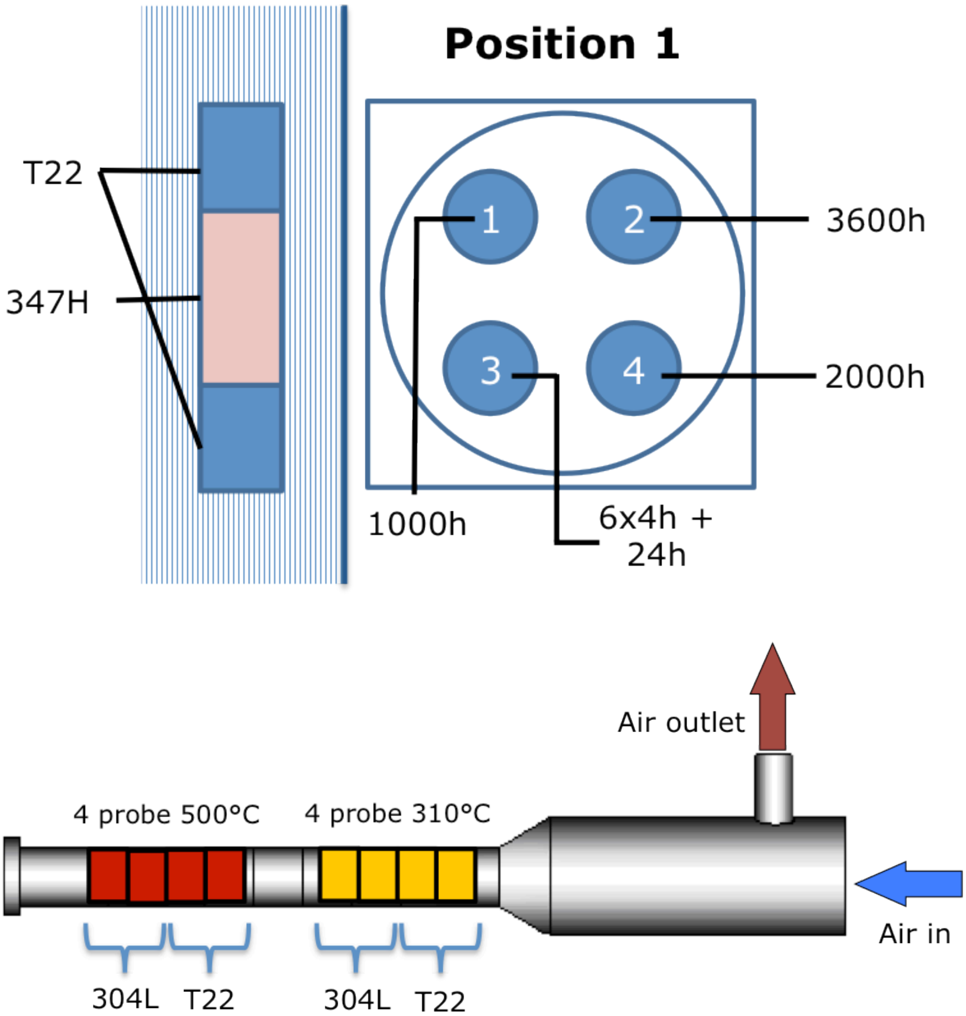


**Figur 9. Skiss på placering av sonder i position 1 samt materialtemperaturer på sonden.**

***Figure 9. Schematic sketch of probes at position 1 and material temperatures on the probes.***

### 3.2.2.2 Position 2

At position 2 long-term exposures were performed. The man hole had 2 openings. Opening 1 was used for 3600 hours exposure and opening 2 for 1000 hours exposure, see Figure 10.

In these exposures, isothermal probes were also used. A total of 6 rings were placed on the probes. The materials used were 347H, 304L and T22. The following figure shows a schematic sketch of the probe. The material tubes were placed close to cooled probes at position 2. The tube probe is similar as the one at position 1, see Figure 10.

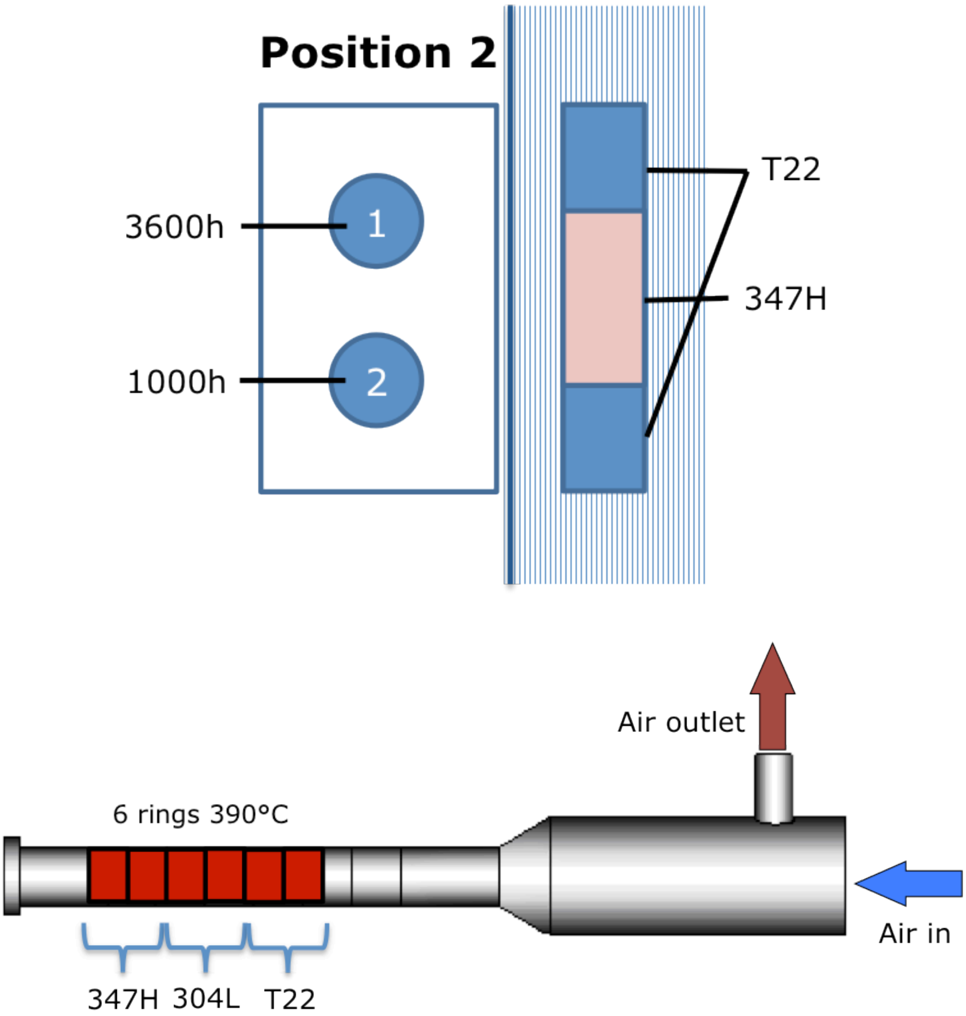


**Figur 10. Skiss på placering av sonder i position 2 samt materialtemperaturer på sonden.**

***Figure 10. Schematic sketch of probes at position 2 and material temperatures on the probes.***

### 3.2.3 Evaluation of probe and tube samples

#### 3.2.3.1 Short-term exposures

Qualitative corrosion analyses of the probe samples

All the samples were investigated by visual inspection after exposure. Optical images were taken from the windward side. Color, thickness and adherence of the deposit material give rough information of the overall condition and performance of the exposed sample. In the case of long-term exposures some samples were mounted in epoxy for analysis by SEM/EDX and material loss calculation.

Gravimetric analysis and loose material calculation

All rings were cleaned in acetone and ethanol in ultrasonic bath. The rings were weight before and after exposure using a 5 decimal Sartorius™ balance. Due to spallation and loss of deposit material, the measuring faults of the samples mass gain may be high.

In the case of loose material calculation, the exposed rings were tested with a simple method. The method consists in dropping the exposed ring from a specific position and stops it suddenly. The loose deposit from the ring falls off and is collected and weight. Based on mass gain of the ring, the percentage of loose materials is calculated. This method have been presented earlier in the waste refinery project [19].

X-ray diffraction

In order to determine the crystalline phases in the deposit and corrosion layer, XRD was used. The diffractometer was a Siemens D5000 powder difractometer, equipped with grazing – incidence beam attachment and a Göbel mirror. Cu – $K_{\alpha}$ radiation was used and the angle of incidence was 2. The measuring range of the detector was 10°<2<65°.

The deposit from exposed rings was scraped off and ground to obtain a powder with uniform size. Part of the deposit powder was used for XRD scanning.

Ion chromatography

In order to determine the amount of water-soluble anions ($Cl^-$ and $SO_4^-$) Dionex 100 system was used. The anions were analysed with an Ion Pac AS4A-SC analytic column and 1.8 mM $Na_2CO_3$/1.7mM $NaHCO_3$ was used as eluent. The flow rate was 2ml/min.

The deposit material was weighted and leached in 50ml of MilliQ water. The leached powder solution was filtered to dispose any big particle. The new powder solution was diluted in MilliQ water till the concentration reached the required range for the equipment.

The final solution was analysed and compared against different pattern solutions in order to calculate the amount of chloride and sulphate anions in the powder solution.

ICP-OES

Deposit powder was weighted and leached in 50ml of water. The solution was filtered. The collected solids were leached in $HNO_3$ (1M). The solution was diluted in $HNO_3$ till the concentration reached the required range for the equipment. The filtered solution was also analysed.

3.3.1.2 Long-term exposures

As mentioned long-term exposures were performed in different positions. The exposed rings and tubes were handled the same way for analysis. Besides SEM/EDX and material loss calculation, long-term exposure deposit were analysed by XRD.

Scanning electron microscopy

The morphology of samples scale was investigated by scanning electron microscopy (SEM). Since the resolution and depth of focus in a SEM is higher than in an optical microscope more details of the corrosion attack can be revealed. In addition, energy dispersive X-rays (EDX) system is used to enable elemental composition analysis of the sample. The samples were analysed with a FEI Quanta 200 FEG ESEM. The SEM has a field emission electron gun (FEG) and is equipped with an Oxford energy dispersive X-ray system. For imaging and EDX analysis accelerated voltage of 20-25kV was used.

Long-term samples were embedded in epoxy resin and cut with a water free cooling liquid. After cutting, rings were dry ground till 4000 grit. Since the rings were embedded in epoxy, gold coating was necessary prior to SEM/EDX analysis.

Material loss calculation

All long-term exposed samples were evaluated by means of material loss determination. The wall thickness of the material rings was measured with micrometer before exposure. The wall was measured in 8 different points. In the case of tube probes, they were compared against the nominal thickness.

After exposure, wall thicknesses measured using cross-sectional samples. Wall thicknesses were measured with SEM. Measurements were done in 12 different locations along the ring, rotating the ring every 30° clockwise.

# 4 Results

## 4.1 Short-term probe exposures

The aim of the short-term exposures is to follow changes in deposit formation over time, including deposit growth rate, deposit composition and correlations between the deposit and flue gas chemistry. 8 steel rings were mounted onto the probe in each test run before it was introduced into the boiler. The probe has two temperature zones and according to the temperature controllers the average values were 304°C and 455°C.

The samples were exposed when the boiler at least had a load of 80%. Before and after exposure the sample weights were recorded in order to calculate the mass gain rate. Table 6 compiles exposure data and obtained mass gain for the short term exposures at SH2 in boiler P6, Högdalen.

| Date | Exposure time (h) | Material | Material temperature (°C) | Mass gain ($g/m^2*h$) |
|---|---|---|---|---|
| 12-Oct-2012 | 04:00 | 304L | 450 | 4,7 |
| | | | 303 | 2,0 |
| | | T22 | 450 | 7,1 |
| | | | 303 | 6,2 |
| 29-Oct-2012 | 04:00 | 304L | 443 | 31,8 |
| | | | 306 | 10,5 |
| | | T22 | 443 | 45,5 |
| | | | 306 | 26,2 |
| 20-Nov-2012 | 04:00 | 304L | 486 | 29,8 |
| | | | 307 | 5,6 |
| | | T22 | 486 | 39,4 |
| | | | 307 | 19,4 |
| 2-Jan-2013 | 04:00 | 304L | 470 | 86,3 |
| | | | 301 | 9,3 |
| | | T22 | 470 | 82,5 |
| | | | 301 | 16,3 |
| 7-Feb-2013 | 04:00 | 304 | 440 | 24,0 |
| | | | 303 | 6,2 |
| | | T22 | 440 | 17,9 |
| | | | 303 | 12,9 |
| 8-Mar-2013 | 04:00 | 304L | 443 | 19,6 |
| | | | 304 | 8,1 |
| | | T22 | 443 | 17,0 |
| | | | 304 | 18,1 |

**Table 6. Exposure data and obtained mass gains for the short term exposures.**

The Figure 11 shows the mass gain of the samples exposed for 4 hours. The samples exposed at the higher material temperature, i.e. 455 °C, show a higher mass gain compared to the samples exposed at the lower temperature (304 °C). For the samples exposed at 455 °C, the mass gains are more scattered between the different exposures compared to the samples exposed at 304 °C.

By comparing the mass gains for T22 and 304L it can be noted that T22 in general exhibits a higher mass gain. Since the mass gain is due to both deposit formation and the formation of corrosion products, the higher mass gain for T22 may be attributed to a more severe corrosion attack.

The exposure “12 October” was performed directly after the boiler started up after revision and the altered deposit formation in the boiler due to large areas of clean surfaces is expected to have influenced the mass gain of the samples.

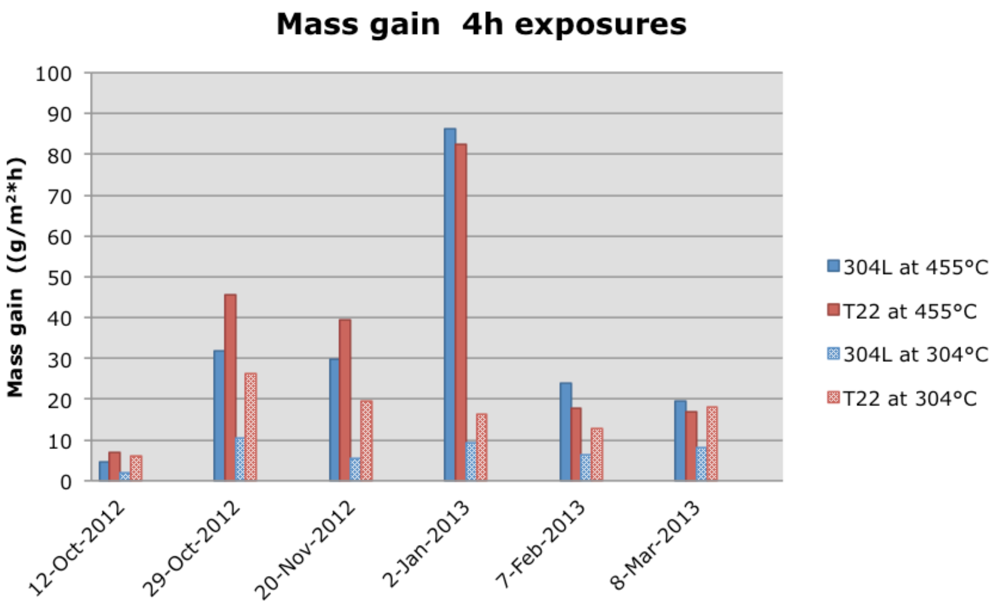


**Figur 11. Massökning för T22 och 304L efter korttidsexponeringarna.**

***Figure 11. Mass gain for T22 and 304L after the short term exposures.***

Figure 12 shows optical images of the short term exposed samples. In general, the sample rings exhibited an uniform beige/greyish deposit covering the surface. At 455 °C, the deposit layer was slightly thicker compared to the samples exposed at 304 °C. This is especially pronounced for the wind side of the samples. However, at the higher temperature, the T22 samples showed signs of spallation on a majority of the exposed samples. At 304° C, no spallation was observed. The extent of spallation can usually be correlated to the extent of corrosion; the corrosion product layer induces poor adherence to the underlying steel bulk.

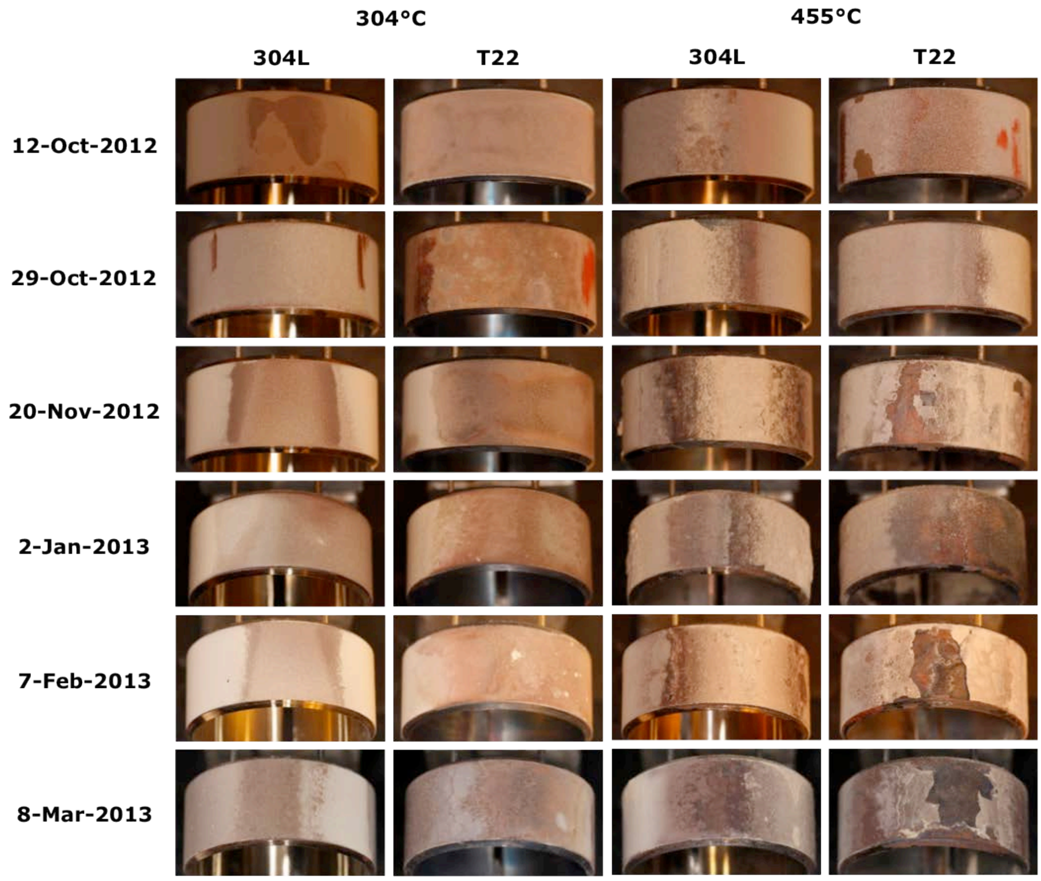


**Figur 12. Optiska bilder av provringar exponerade vid 304 och 455 °C i 4 timmar.**

***Figure 12. Optical images of the samples exposed for 4 hours at 304 and 455 °C.***

In order to investigate how much of the deposit that were of loose, non sticky character a loose material test, described in section 3.2.3.1, was performed. Since the T22 samples suffered from severe spallation where large flakes of deposit and corrosion products were spalled off, only the 304L samples were investigated by means of the loose deposit test.

The results of the loose deposit test performed on the 304L samples are shown Figure 13. In general the adherence of the deposit to the sample surface was good. The fraction of loose deposit was only about 5% for the samples exposed at 304 °C and about 10% for the samples exposed at 455 °C. This correlates well with the optical images of the rings, showing an uniform and adherent deposit on the 304L sample rings.

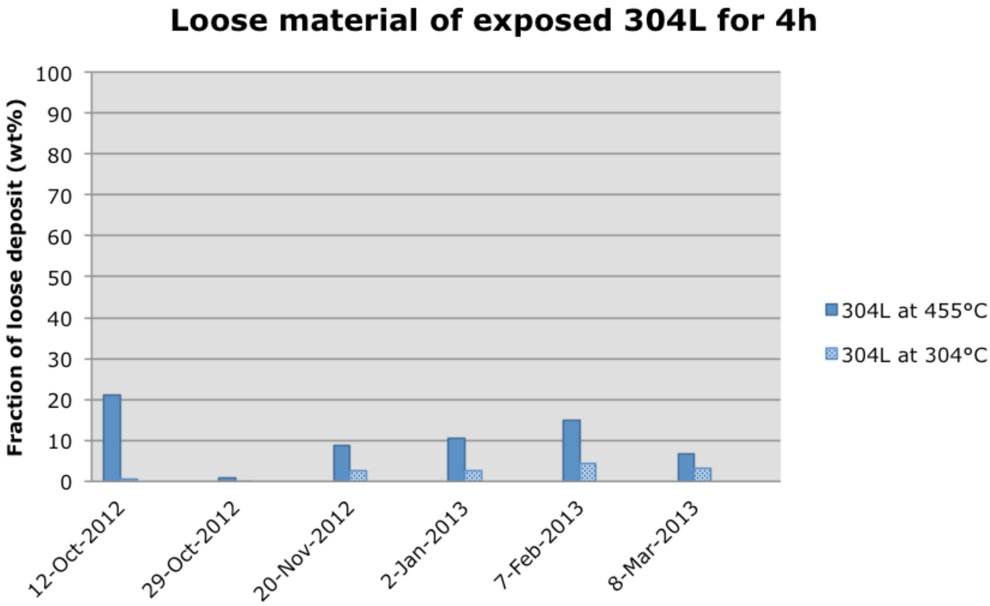


**Figur 13. Procent lössittande avlagring på 304L proverna i korttidsförsöken.**

***Figure 13. Fraction of loose deposit on 304L for the short term exposures.***

In order to characterize the deposit composition, some deposit was scraped off from the surface of all exposed rings. The deposit material was analysed with IC in order to determine the amount of Cl and S present. Furthermore, ICP-OES analysis was performed on the deposit material in order to quantify the amount of other elements in the deposit.

In the following figures (Figure 14 - Figure 16) the results from the IC and ICP-OES analyses of the deposits are shown. In Figure 14, the amounts of chlorine and sulphur, detected by IC, are plotted together with the amounts of chlorine and sulphur in the fuel. The deposit chlorine and sulphur are measured in wt% of analyzed deposit whereas the chlorine and sulphur content of the fuel is measured in %TS (=% of dry substance). For both chlorine and sulphur, the %TS in the fuel varies between 0.3 - 1.0. The average values of chlorine and sulphur for all 6 fuel anlaysis are 0.51 and 0.57 %TS, respectively. Compared to the fuel analysis, the fraction of these species in the deposit is increased, the average values being 9.0 and 3.87 wt% of the deposit, respectively. Thus, the precentage of chlorine is increased about 17 times and for sulphur about 4 times, comparing the fractions in the deposit with the fuel. With the exception of a few points, the curves of both chlorine an sulphur indicates that there exists a correlation between the deposit and fuel fractions, higher concentration in the fuel leads to higher concentration in the deposit. This indicates that the interaction between the flue gas and deposit previously formed on boiler walls etc is minor.

Since Calcium is known for greatly affecting the sulphur chemsitry in the boiler, the fractions of Calcium in both the fuel and the deposit is shown Figure 14. Similar to chlorine and sulphur, the two fractions (i.e. fuel and deposit fractions) correlates well. However, in contrast to chlorine and sulphur, the fraction of calcium in the fuel is much higher, being around 2.1 TS% (compared to about 0.5% for chlorine and sulphur). Furthermore, calcium does not appear to form fly ash/deposit to equally high degree as chlorine and sulphur, the ratio between deposit and fuel fractions is only 5.2 (compared to around 17 for chlorine and 4 for sulphur).

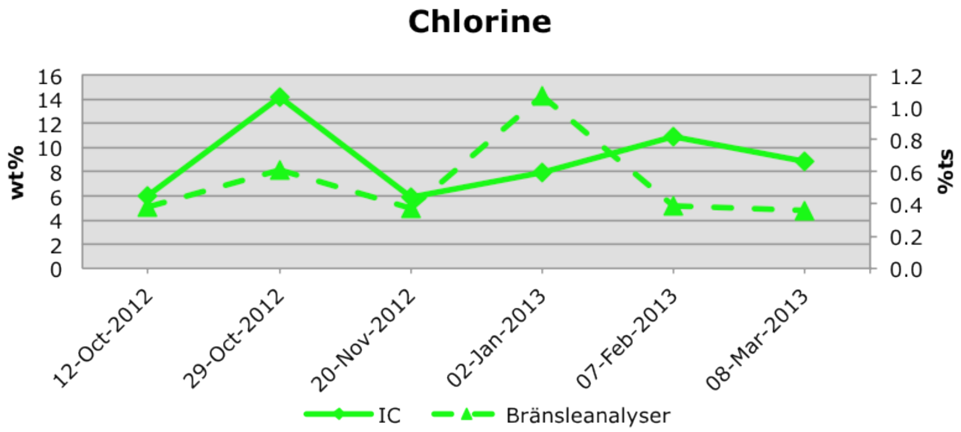


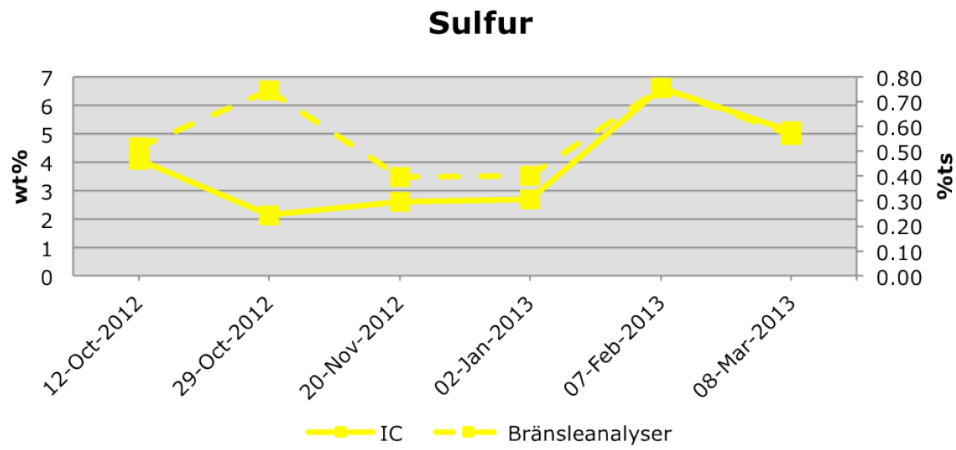


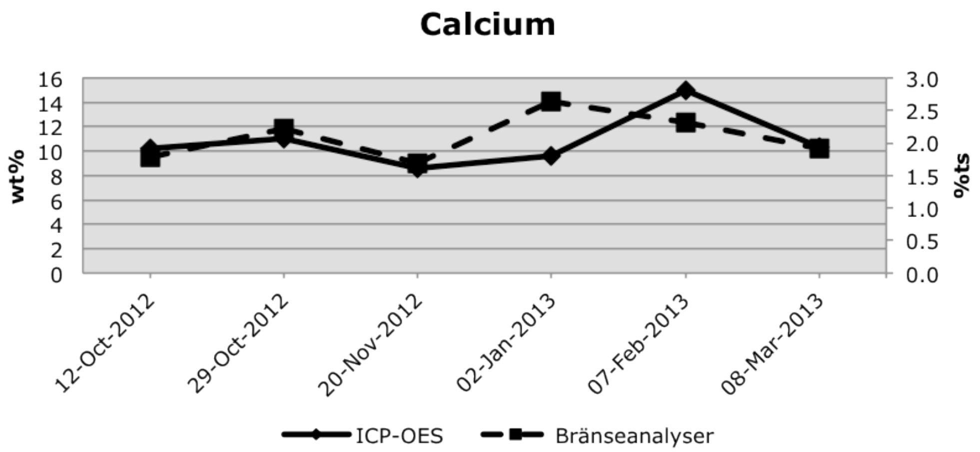

**Figur 14. Fraktioner av klor, svavel och calcium i bränsle och avlagringar uppmätta för 304L exponerad vid 455 °C i 4 timmar.**

***Figure 14. Fractions of chlorine, sulphur and calcium measured in the fuel and the deposit formed on 304L exposed at 455 °C for 4 hours.***

In Figure 15, the S/Cl ratio in the flue gas is compared to the S/Cl ratio in the deposit formed on 304L exposed at 455 °C for 4 hours. As the results show, there is a strong correlation between the sulphur to chlorine ratios in the flue gas and deposit. However, compared to the flue gas, sulphur seems to be enriched in the deposit, the S/Cl ratio in the deposit is a factor of 5 times higher compared to the S/Cl ratio in the flue gas.

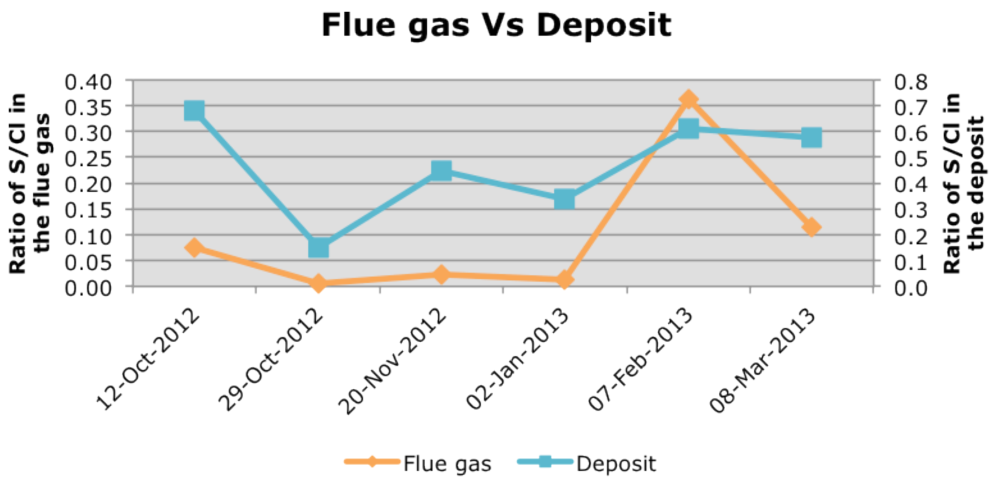


**Figur 15. Jämförelse av S/Cl ratio för rökgasen och avlagringen som bildats på 304L exponerad vid 455 °C i 4 timmar.**

***Figure 15. Comparison between the S/Cl ratios of the flue gas and the deposit formed on the 304L samples exposed at 455 °C for 4 hours.***

In Figure 16, the ICP-OES analyses of the deposit formed on 304L samples exposed at 304 °C and 455 °C for 4 hours is shown. The analyses were performed on 1 gram of deposit and are presented in mol%. In addition, the amounts of chlorine and sulphur, analyzed by ion chromatography, is added to the graph. The dominating elements in the deposit are Ca, Cl and S, regardless of temperature. In addition, Fe, Na and K is detected in lower amounts. At the lower temperature, the presence of small amounts of Zn is noticed.

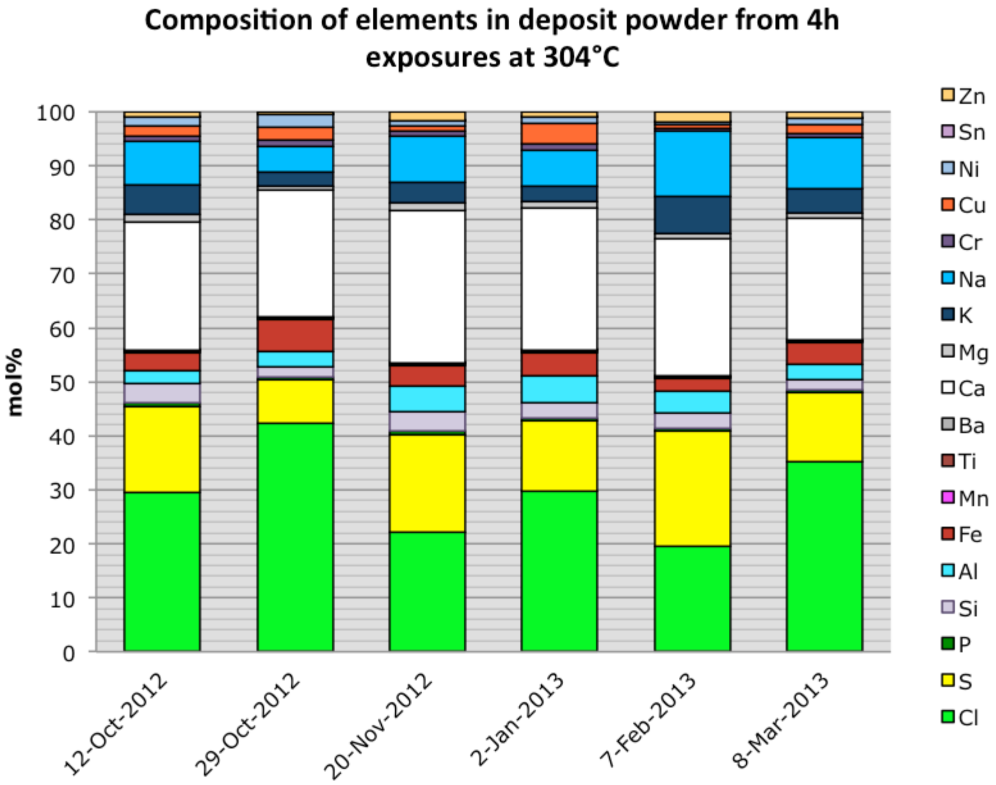
Composition of elements in deposit powder from 4h exposures at 304°C
mol%
100
90
80
70
60
50
40
30
20
10
0
12-Oct-2012
29-Oct-2012
20-Nov-2012
2-Jan-2013
7-Feb-2013
8-Mar-2013
Zn
Sn
Ni
Cu
Cr
Na
K
Mg
Ca
Ba
Ti
Mn
Fe
Al
Si
P
S
Cl

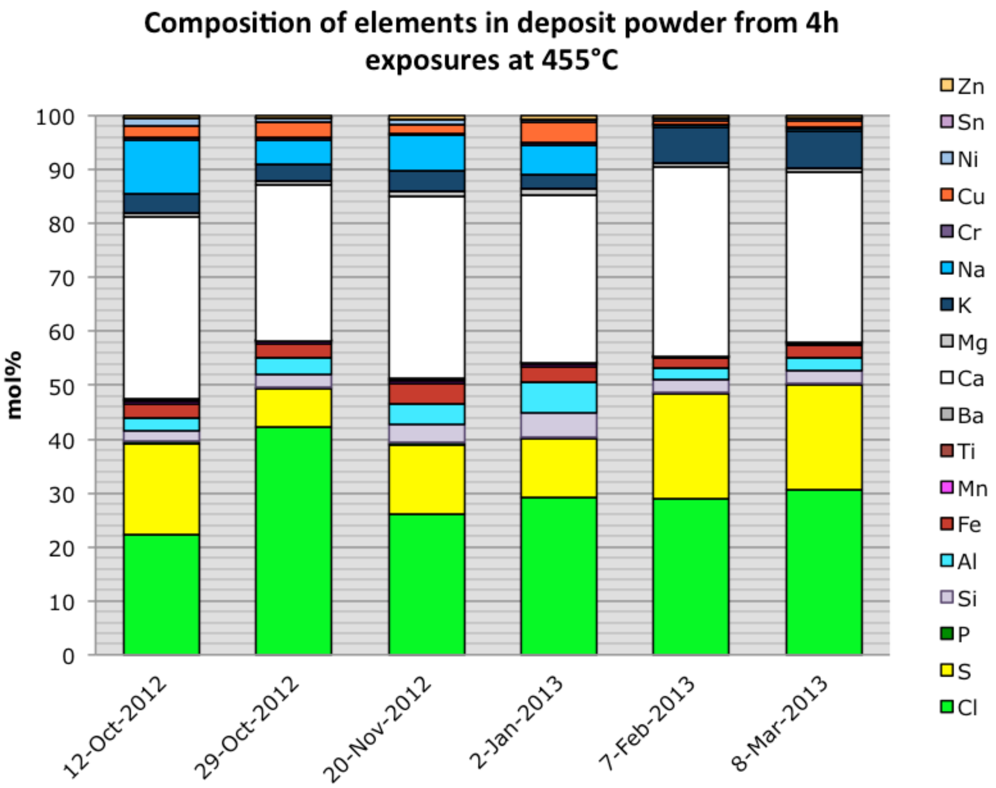
Composition of elements in deposit powder from 4h exposures at 455°C
mol%
100
90
80
70
60
50
40
30
20
10
0
12-Oct-2012
29-Oct-2012
20-Nov-2012
2-Jan-2013
7-Feb-2013
8-Mar-2013
Zn
Sn
Ni
Cu
Cr
Na
K
Mg
Ca
Ba
Ti
Mn
Fe
Al
Si
P
S
Cl

**Figur 16. Avlagringssammansättning på 304L-prov exponerade i 4 timmar vid 304 °C och 455 °C analyserade med IC och ICPOES.**

***Figure 16. Composition of the deposit formed on the 304L samples exposed at 304 °C and 455 °C. Analysis by IC and ICPOES.***

IC and ICPOES was used for analyzing the deposit composition in a quantitaive manner. In order to analyze the deposit from a qualitative manner, XRD was performed. With XRD, the crystalline phases present in the deposit can be analyzed, see Table 7 for the 304L samples exposed for 4 hours at 304 °C and 455 °C. For all samples, the dominant phase present in the deposits is $CaSO_4$, which agrees with the IC and ICP-OES results. In addition, corrosion products in the form of $Fe_2O_3$, spinel type oxide ($Me_3O_4$) and $FeCl_2x2H_2O$ were detected. Hence, the 304L samples exposed for 4 hours have started to corrode. From XRD it is hard to distguinish the exact composition of the spinel type oxide since many types of spinel oxides (e.g. $Fe_3O_4$, $(FeCr)_3O_4$ and $(FeCrNi)_3O_4$) overlap. Besides $CaSO_4$, the deposit is also containing alkali chlorides (i.e. NaCl and KCl). There is a tendency that KCl is dominating at 455 °C and NaCl at 304 °C.

| Exposure date | Temperature (°C) | $CaSO_4$ | $Fe_2O_3$ | $Me_3O_4$ | KCl | NaCl | $FeCl_2$ x2$H_2O$ |
|---|---|---|---|---|---|---|---|
| 12-Oct-2012 | 455 | S | S | S | W | | W |
| | 304 | S | S | | | | S |
| 29-Oct-2012 | 455 | S | S | S | | M | M |
| | 304 | S | S | | W | M | S |
| 20-Nov-2012 | 455 | S | S | S | M | | W |
| | 304 | S | S | | | M | M |
| 2-Jan-2013 | 455 | S | S | S | M | | |
| | 304 | S | S | | | M | W |
| 7-Feb-2013 | 455 | S | | M | M | | |
| | 304 | S | S | | | M | |
| 8-Mar-2013 | 455 | S | M | S | W | M | |
| | 304 | S | S | | M | S | |

Intensity of peaks: S=strong; M=medium; W=weak

**Table 7. X-ray diffraction results of deposit material from 304L short exposures.**

## 4.2 Long-term exposures

Long-term exposures were performed in order to observe the corrosion rate over time, but also to compare the results from cooled probes and test sections of the superheater. The probes were mounted during revision at the same time as the test sections of the superheater were installed. The exposure times of the probes were 24, 1000, 2000 and 3600 hours. The exposure time of the test sections was 3600 hours.

Optical images of long-term exposed sample rings are showed in Figure 17. After 24 hours the rings have an uniform beige deposit layer. In the case of T22, spallation is occurring, especially on the windward side. On the samples exposed for 1000 hours a thick beige deposit has formed. The deposit layer is thicker on the windward side. In general, the deposit formed after 1000 hours is adherent to the sample rings. After 2000 hours, the deposit layer has grown in thickness. However, the samples exposed at 455 °C have suffered from spallation, which can be seen in Figure 17 where most of the deposit has been lost on both 304L and T22 at this temperature. In the areas where the where deposit has spalled off, the corrosion products are seen as red and grey layer. The poor adherence of the deposit layer is also seen for the samples exposed at 455 °C for 3600 hours. At 304 °C, however, the adherence of the deposit layer is much better and no signs of spallation can be seen, regardless of exposure time. The effect of material temperature is evident by optical inspection. At 304 °C, a beige, thick and adherent deposit layer have formed on the samples. At 455 °C, the deposit material has spalled off after longer exposures times especially at the windward side. Underneath the deposit, red dark grey areas are seen. Red areas dominate the surface of T22 rings where the deposit has been lost indicating the presence of hematite.

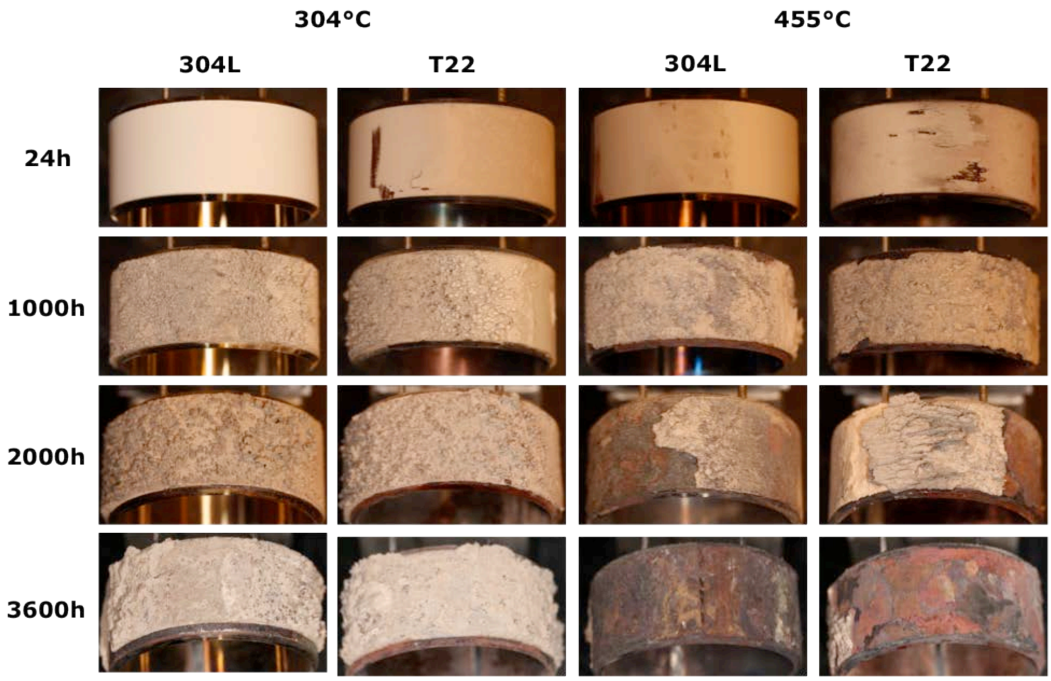


**Figur 17. Optiska bilder av T22 och 304L exponerade på sonder i 24, 1000, 2000 samt 3600 timmar vid 304 och 455 °C i position 1 (före överhettare 2).**

***Figure 17. Optical images of T22 and 304L samples exposed on probes for 24, 1000, 2000 and 3600 hours at 304 and 455 °C at position 1 (before superheater 2).***

Optical images of the samples exposed at position 2 (i.e. after superheater 2) are shown in Figure 18. In this position, 347H, 304L and T22 were exposed at 390 °C for 1000 and 3600h. In similarity to the samples exposed at 455 °C at position 1, spallation has occurred on all samples. The remaining deposit is beige and relatively thin compared to the samples exposed at position 1, especially on the sample rings exposed for 1000h. Corrosion products can be seen on parts with spallation as red/brown areas.

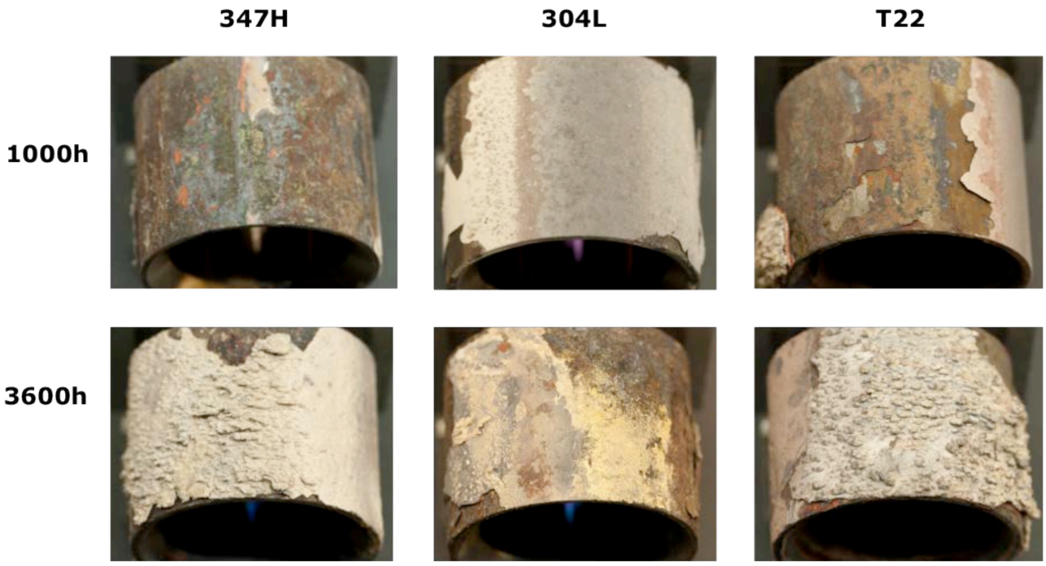


**Figur 18. Optiska bilder av 347H, 304L och T22 exponerade på sonder i 1000 och 3600 timmar vid 390 °C i position 2 (efter överhettare 2).**

***Figure 18. Optical images of 347H, 304L and T22 samples exposed on probes for 1000 and 3600 hours at 390 °C at position 2 (after superheater 2).***

In addition to probe exposures, test sections were installed in the beginning and end of the superheater bundle as close as possible to position 1 and 2, respectively. These tubes were exposed for 3600h. The material temperature of the test tubes installed closest to position 1 was 310 °C and closest to position 2 was 390 °C. Optical images of the tube samples are shown in Figure 19.

The test tubes closest to position 1 have a relatively thick beige deposit but also signs of spallation. Beneath the deposit layer, grey and red areas are visible indicating the presence of a corrosion product layer. In the case of the 347H tube sample, part of the corrosion product layer is green in color, indicating the presence of metal chlorides.

The tube samples exposed in the end of the superheater (i.e. position 2) has lost all deposit. The surface underneath the deposit is completely visible. On the 347H sample beige, grey and somewhat red areas can be observed. On the T22 sample the corrosion product layer is dominate by red.

According to the optical inspection of the tubes it was concluded that the tube samples in general were mildly corroded. The most corroded area was located at the windward side.

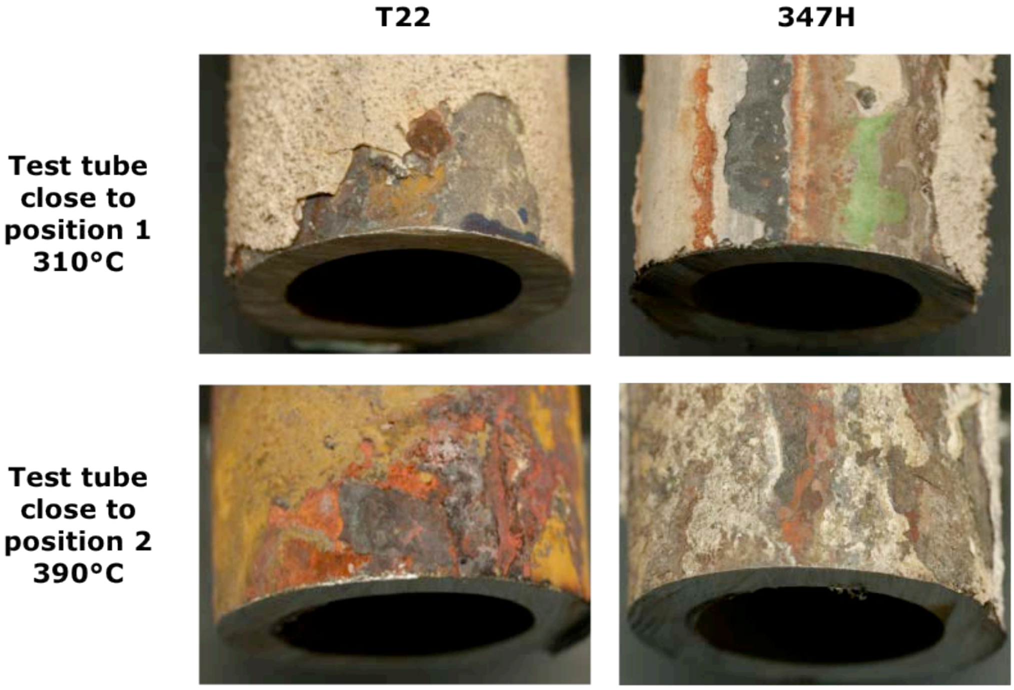


**Figur 19. Optiska bilder av T22 och 347H testtubsprover exponerade i 3600 timmar vid 310 °C och 390 °C, motsvarande i position 1 och position 2.**

***Figure 19. Optical images of 347H, 304L and T22 samples exposed on probes for 1000 and 3600 hours at 310 °C and 390 °C, at position 1 and position 2 respectively.***

In order to get a better understanding of the corrosion behavior of the probe samples, material loss evaluation of the exposed samples was performed. Prior to the material loss calculation optical analysis of the cross section was performed, see Figure 20. The most affected area of the probe exposed samples was, in similarity to the tube exposed samples, the windward side.

The 304L samples show a smooth seemingly unaffected surface around the sample ring. However, at a closer look at the samples exposed for 2000 and 3600h, localized corrosion can be seen in the form of pits. Compared to 304L, the T22 samples exhibit a slightly rougher surface; the corrosion attack is more uniform and not localized as in the case of 304L.

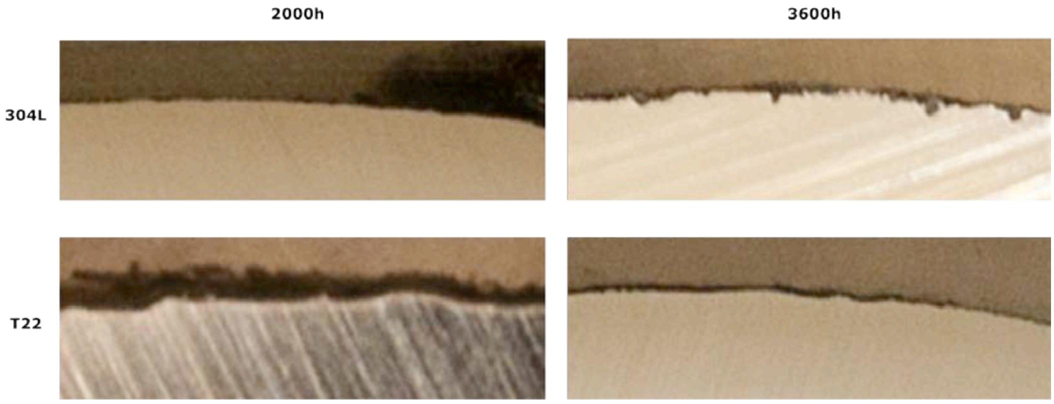


**Figur 20. Optiska bilder av tvärsnittet av 304L och T22 exponerade på sonder i 2000 och 3600 timmar vid 455 °C i position 1.**

***Figure 20. Optical images of cross section from long-term exposed 304L and T22 rings (position 1) at 455 °C.***

The cross sections of the samples seen in Figure 20 were used for material loss calculation by measuring the thickness of the sound metal in the SEM. For each sample 12 measuring points were performed and compared to the original thickness. In Figure 21 the average value of the material loss for these 12 points is presented.

In general, the measured corrosion rates are rather small for all samples, see Figure 21. The majority of data points lie below 0.1 mm, regardless of material, material temperature or exposure time. In fact, only 347H exposed for 3600 hours at 390 °C exhibit a material loss slightly greater than 0.1 mm, the material loss being 0.16 mm. In many cases, the deviation between different materials and exposure times is within the margin of error for this measuring technique, about ±0.03mm. However, as seen on the optical cross sections in Figure 20, the T22 sample exposed for 2000 hours at 455 °C showed higher degree of corrosion which can be seen in the material loss graph in Figure 21. Even though 304L and T22 exhibit similar corrosion rates, the corrosion attack of the two steels is different. In the case of 304L, the average corrosion rate is primarily because of the localized corrosion attacks. For the T22, the corrosion is more general and thus, a dominating part of the corrosion rate comes from this, rather uniform corrosion.

The observed corrosion is in line with the current situation of the installed SH2 in P6; the corrosion rate of the superheater is low. Until now, the current lifetime of the superheaters is 14 years.

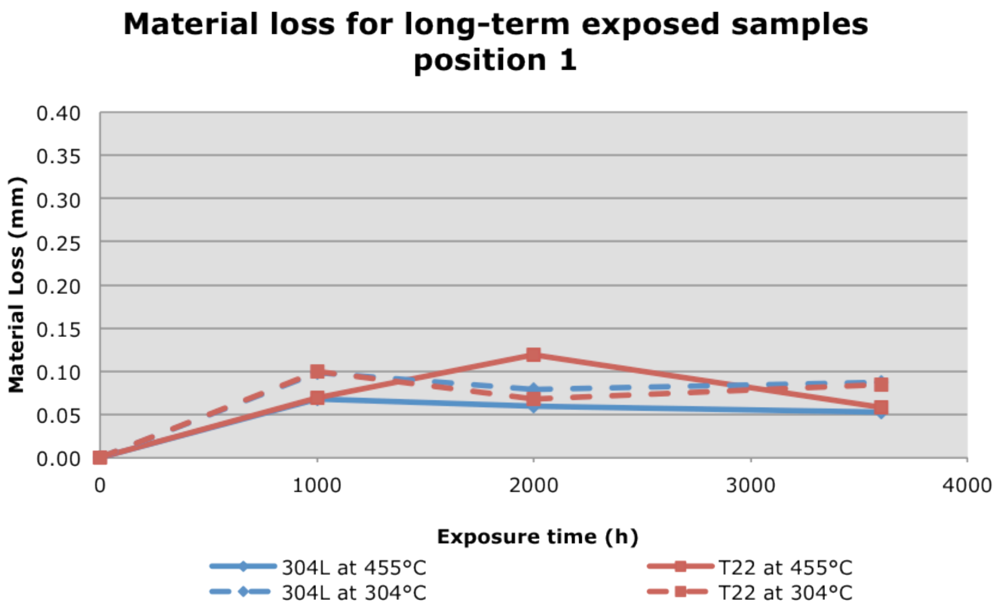


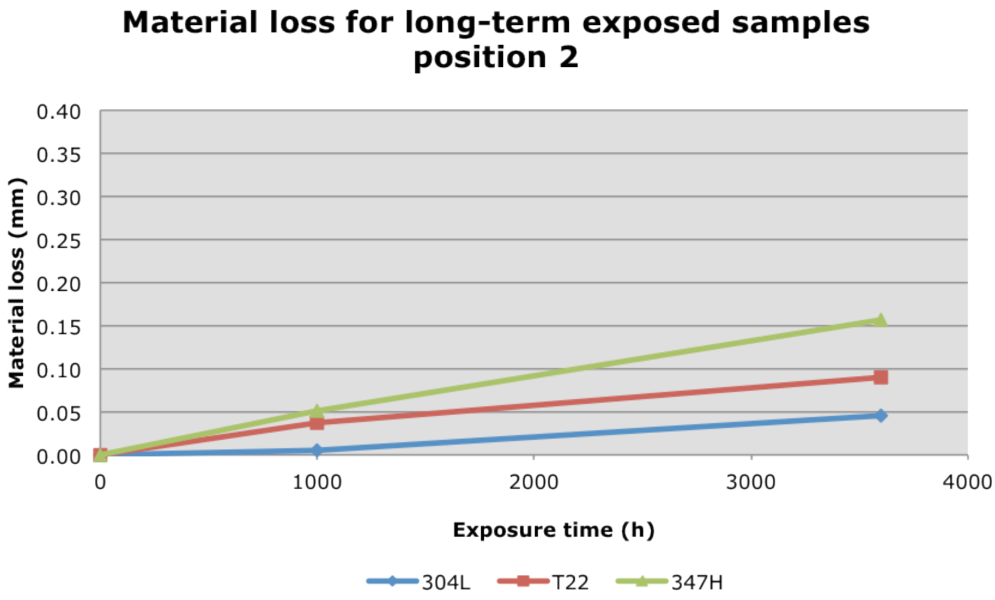


**Figur 21. Materialförlust i mm versus exponeringstid. Övre diagrammet: T22 och 304L exponerade på sond vid 304 °C och 455 °C i position 1 (före överhettare 2). Nedre diagrammet: T22, 347H och 304L exponerade på sond vid 390 °C i position 2 (efter överhettare 2)**

***Figure 21. Material loss in mm versus exposure time. Top graph: T22 and 304L exposed on a probe at 304 °C and 455 °C at position 1 (before superheater 2). Bottom graph: T22, 347H and 304L exposed on a probe at 390 °C at position 2 (after superheater 2).***

In order to see the progress of the corrosion rate over time, the corrosion rate (in mm/year) versus exposure time is presented for the exposed probe samples at position 1 in Figure 22. As can be seen, the corrosion rate decreases with time, from maximum about 0.9 mm/year after 1000 hours to about 0.2 mm/year after 3600 hours.

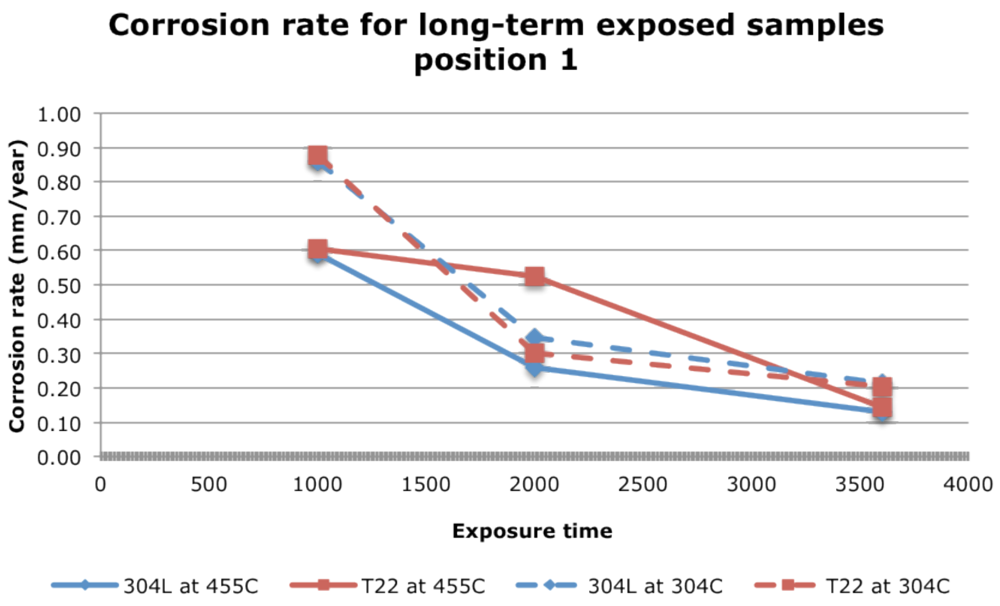


**Figur 22. Materialförlust i mm/år versus exponeringstid för T22 och 304L prover exponerade på sond vid 304 °C och 455 °C i position 1 (före överhettare 2).**

***Figure 22. Material loss in mm/year versus exposure time for T22 and 304L samples exposed on a probe at 304 °C and 455 °C at position 1 (before superheater 2).***

One of the goals of the long-term exposures was to compare the corrosion rate of air-cooled probes and tubes inside the boiler. Hence, test sections of the superheater bundle were installed during revision. One location of the test sections was close to the probes at position 1 and the other location was close to the probes at position 2. The material temperature of the installed test section close to position 1 was ~310 °C. The material temperature of the probe samples at position 1 were ~304 °C. The material temperature of the installed test section close to position 2 was ~390 °C, which was the same material temperature as the probe exposed samples.

For both test sections installed in the superheater, 347H and T22 were used as testing materials. These materials are used today as superheater material of boiler P6 at Högdalen. The materials exposed on probes at position 1 were 304L and T22. The reason for choosing 304L instead of 347H was due to lack of correct probe dimensions for the 347H material. The probes at position 2 (which had a different dimension compared to the probes at position 1) were fitted with 347H, 304L and T22 samples.

The comparison between tube and probe exposed samples for position 1 and position 2 is shown in Figure 23. For reasons presented earlier, the probe at position 1 was fitted with 304L samples whereas the tube test section was fitted with 347H. By comparing these samples, it can be seen that the corrosion rate is higher for the probe exposed 304L sample compared to the tube exposed 347H. However, the corrosion is for both materials minor. The comparison of T22 tube and probe samples reveals a larger difference; the corrosion of the tube exposed sample is roughly 3 times higher.

For position 2, the probe exposed stainless steels (304L and 347H) exhibits a material loss of 0.05 mm and 0.15 mm, respectively. The material loss of the corresponding tube exposed 347H sample is 0.08 mm. Thus, the difference between probe and tube exposed samples is minor. For T22, the tube exposed sample (with a material loss of 0.18 mm) is about 2 times higher compared to the corresponding probe exposed sample (with a material loss of 0.09 mm). Hence, for position 2 the probe versus tube corrosion is showing opposite behavior compared to position 1, where the tube exposed sample exhibited much higher material loss compared to the probe exposed sample. From these results, no clear trend can be drawn whether there exists an inherent difference between probe and tube exposures with respect to the severity of the corrosion attack. However, lacking this trend it is indicated that no such difference exists.

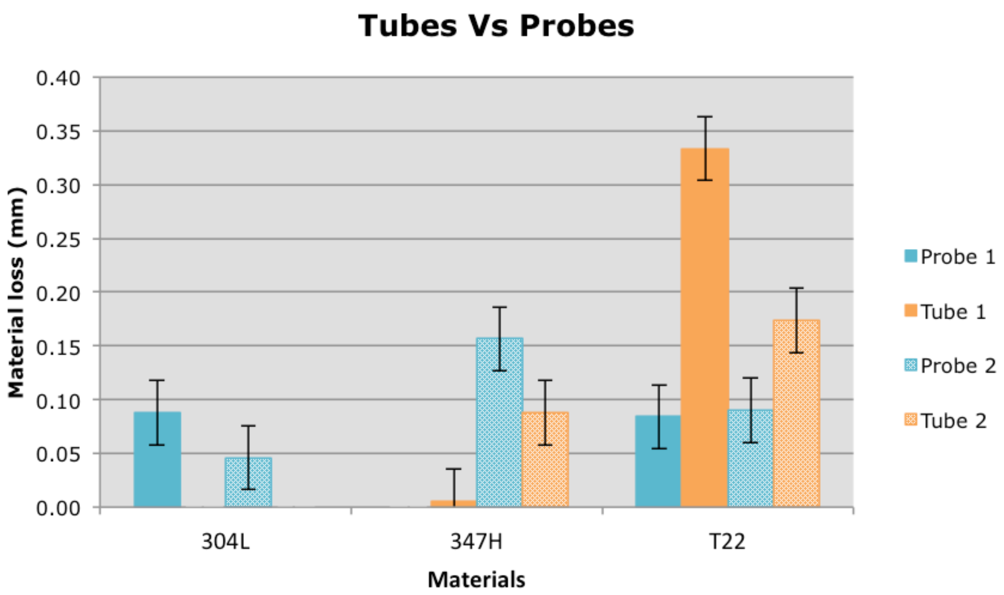


**Figur 23. Materialförlust i mm för 304L, 347H och T22 prover exponerade på sonder och som tubsektioner i position 1 och 2. Materialtemperaturen vid position 1 var ~310 °C och vid position 2 390 °C.**

***Figure 23. Material loss in mm for 304L, 347H and T22 samples exposed on***

***probes and as tubes at position 1 and position 2. The material temperature at position1was ~310 °C and at position 2 the temperature was 390 °C.***

In order to follow the corrosion attack in a more detailed manner SEM analysis was performed on cross sections of probe exposed sample rings at position 1. The following images show the most corroded part of the samples (i.e. the windward side). On the samples exposed for 2000 and 3600h deposit much of the deposit and corrosion product layer was lost during probe outtake. Hence, for some of the SEM images no deposit can be seen.

In Figure 24, T22 and 304L samples exposed at position 1 for 2000 hours at 304 °C and 455 °C is seen. As noticed already in the optical images of the cross sections, the two materials exhibit slightly different corrosion attacks. In the case of T22, the corrosion attack is rather uniform around the sample surface. For 304L, the attack is more localized; most of the sample surface is unattacked but large pits can be seen. The effect of material temperature can be seen in the images as well. For the 304L samples, the higher temperature resulted in much more corrosion in form of pits. In the case of the T22 rings, a porous oxide has formed at both temperatures, however it seems that at the higher temperature the oxide is thicker. However, the corrosion rate is still rather low for both temperatures.

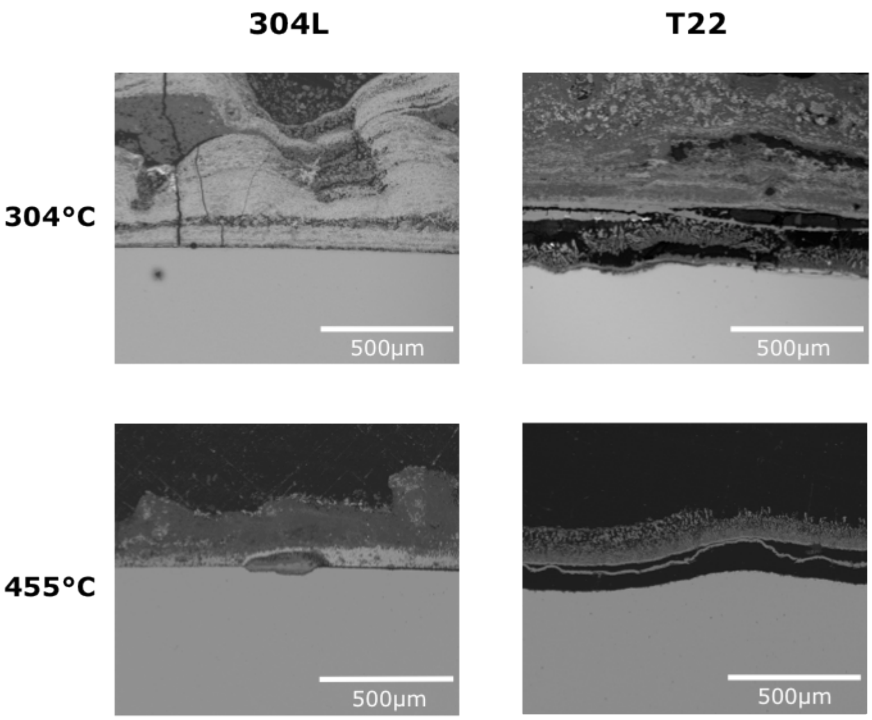


**Figur 24. SEM bilder av tvärsnitt på 304L och T22 exponerade I position 1 vid 304 °C och 455 °C i 2000 timmar.**

***Figure 24. SEM images of the cross sections of 304L and T22 samples***

***exposed at 304 °C and 455°C (position 1) for 2000 hours.***

The SEM examination of the 304L cross sections (at position1) indicated that the main corrosion attack was localized. In Figure 25, the progress of this attack on 304L over time can be seen. Several pits along the ring surface can be observed at all exposure times. The depth and width of the pits increases with exposure time. The deepest pit was detected on the ring exposed for 3600 hours, being approximately 300 μm deep. A dense oxide layer along the metal/oxide interface of the pit can be seen. The corrosion products in the pit display a laminar structure see Figure 25(c). This laminar structure can be observed also for the 1000 and 2000 hour exposed samples. However, not as evident as for the samples exposed for 3600 hours.

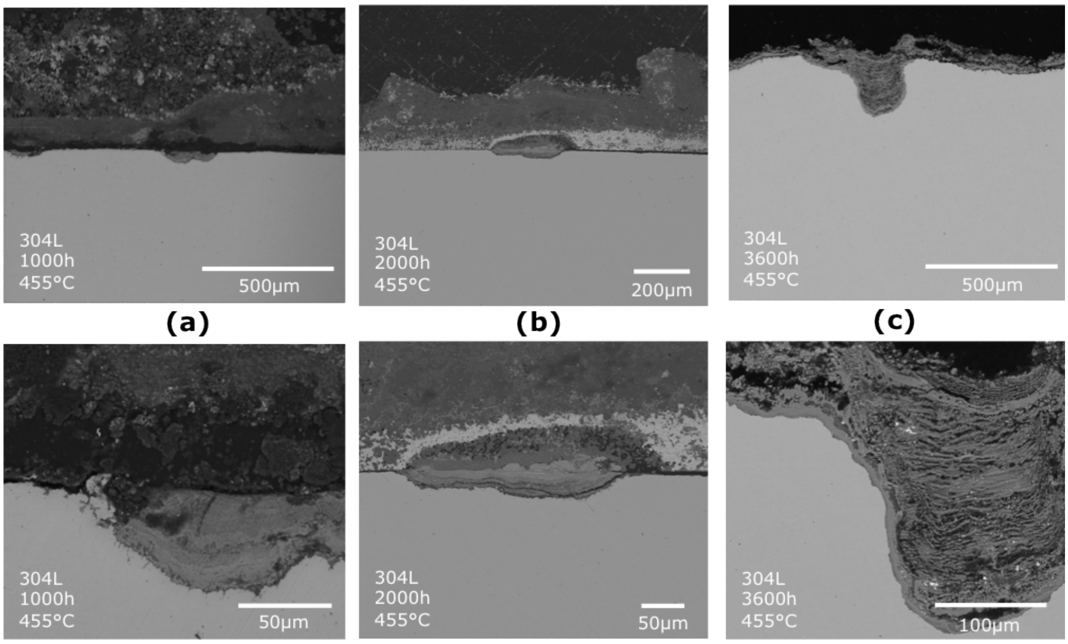


**Figur 25. SEM bilder av tvärsnitt på 304L prov exponerade i position 1 vid 455 °C i (a) 1000 timmar (b) 2000 timmar (c) 3600 timmar.**

***Figure 25. SEM images of cross sections 304L samples exposed at 455°C for (a) 1000h (b) 2000h (c) 3600h.***

In Figure 26 - Figure 28, the results of the EDX analysis of the 304L samples shown in Figure 25 is shown. From the EDX analysis of the 304L sample exposed for 1000 hours (Figure 26), a deposit layer containing K, Na, Ca, O, Cl and S can be seen. The majority of the sample surface beneath this deposit showing little corrosion, the thin oxide formed protects the underlying steel. However, in the middle of the image a much thicker, duplex oxide can be seen. The outer part of the oxide layer is containing Fe and O whereas the inner layer consists of Fe, Cr, Ni and O. The inner part is part is enriched in Cr (the composition of the inner oxide is 27% Cr, 4% Fe, 6% Ni and 54% O). This type of corrosion morphology is often seen the 304L steel after the initial chromium rich oxide have been destroyed; the outer part of the oxide is outward growing $Fe_2O_3$ and the inner part is inward growing spinel type oxide, enriched in chromium but contains also iron and nickel. On the top of this duplex oxide scale traces of potassium, not associated with chlorine or sulphur (even though sulphur also seem to be enriched in the vicinity), can be seen. This might be the remnants of $K_2CrO_4$, known for destroying the protective properties of chromium rich oxide on stainless steels. However, the results are not conclusive. Furthermore, the presence of sulphur can be seen in the outer part of the oxide scale as well as along one side of the inward growing oxide. The inward growing oxide, i.e. the pit, is approximately 20 µm deep.

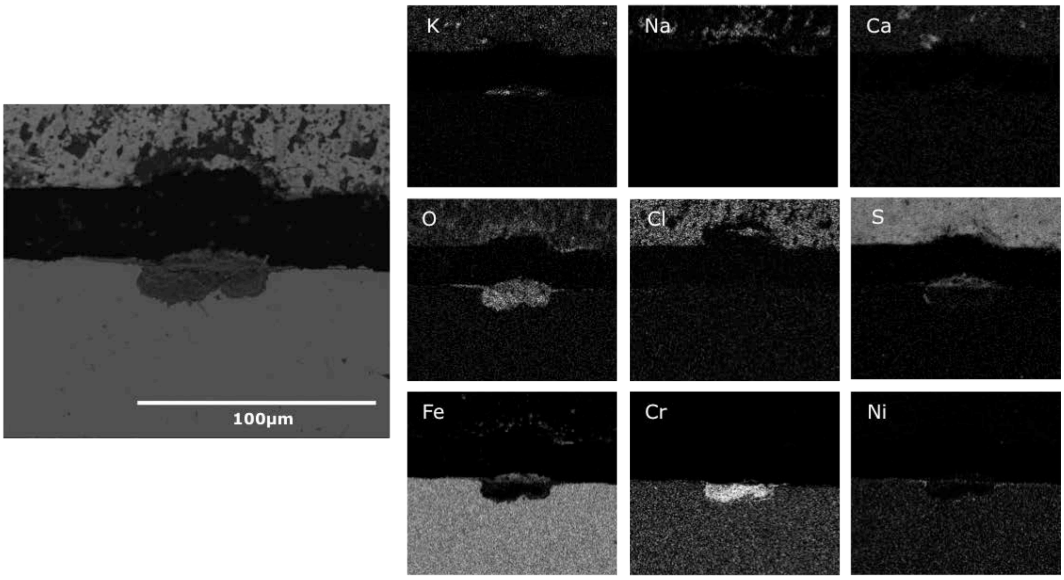


**Figur 26. SEM/EDX analys av ett tvärsnitt av 304L exponerat i 1000 timmar vid 455 °C i position 1.**

***Figure 26. SEM/EDX analysis of a cross section of 304L exposed at 455 °C for 1000 hours at position 1.***

In Figure 27, the SEM/EDX analysis of 304L exposed for 2000 hours is shown. Compared to the sample exposed for 1000 hours, the corrosion attack is similar. However, the corrosion product layer has increased in thickness and width. After 2000 hours, the pit is about 40 µm thick and having a width of approximately 220 µm. The sample surface surrounding the pit is smooth and thin. The composition of the oxide scale is similar as for the 1000 hour exposed sample; the outer part of the oxide is consisting of iron whereas the inner part is enriched in chromium. In this case it seems that once the protective oxide layer breakdown, the Fe diffuses outwards through the chromium rich oxide. Again, a layer of potassium can be detected on top of the duplex oxide scale. After 2000 hours, chlorine is enriched in the metal/oxide interface, probably in the form as metal chloride. Similar to the 1000 hour exposed sample, sulphur can be seen in the oxide scale. The oxide scale is surrounded by deposit material, rich in S, O, Ca, indicating the presence of $CaSO_4$. Other deposit related elements, such as Na, K and Cl were also detected.

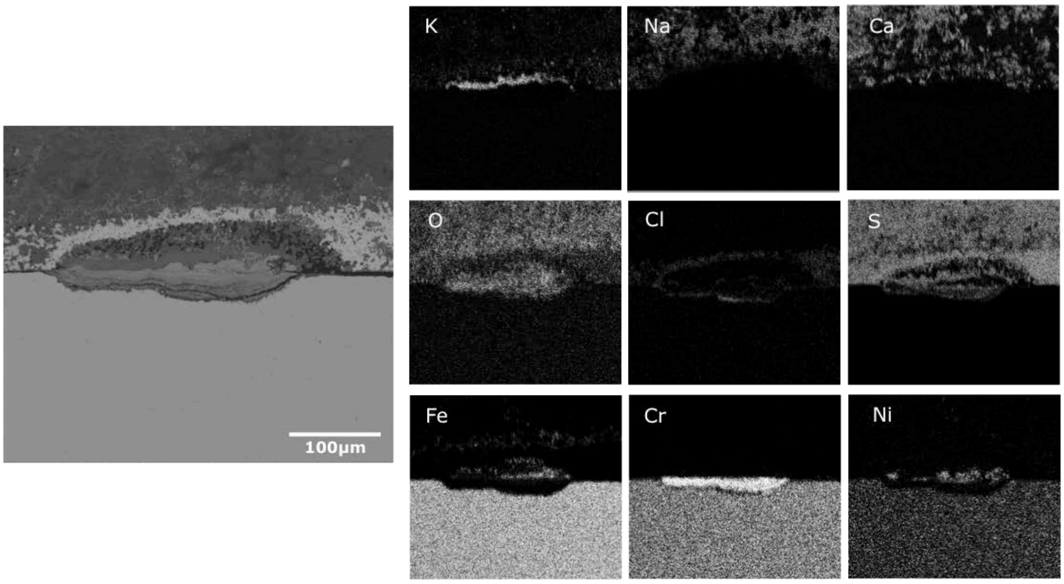


**Figur 27. SEM/EDX analys av ett tvärsnitt av 304L exponerat i 2000 timmar vid 455 °C i position 1.**

***Figure 27. SEM/EDX analysis of a cross section of 304L exposed at 455 °C for 2000 hours at position 1.***

With prolonged exposure times the localized corrosion, i.e. the pits, continues to grow, see Figure 28. For the 304L sample exposed for 3600 hours, the depth of the pit is approximately 200 µm. As for the samples for shorter exposure times, the inward growing oxide layer is showing a laminar structure. These oxide layers are dominated by chromium but contain also nickel and iron (the EDX quantification reveals about equal amounts of nickel and iron). In addition, sulphur and chlorine can be seen dispersed within the pit. Some of these enrichments of sulphur and chlorine is related to alkali (Na or K) or Ca and is probably deposit particles that have been incorporated during sample preparation (i.e. grinding and polishing). However, there are also areas where the presence of these cations is low and thus, it is expected that metal chlorides and metal sulphides have formed. The evolution of these pits and the current composition (i.e. after 3600 hours) do not indicate that the corrosion attack is leveling off.

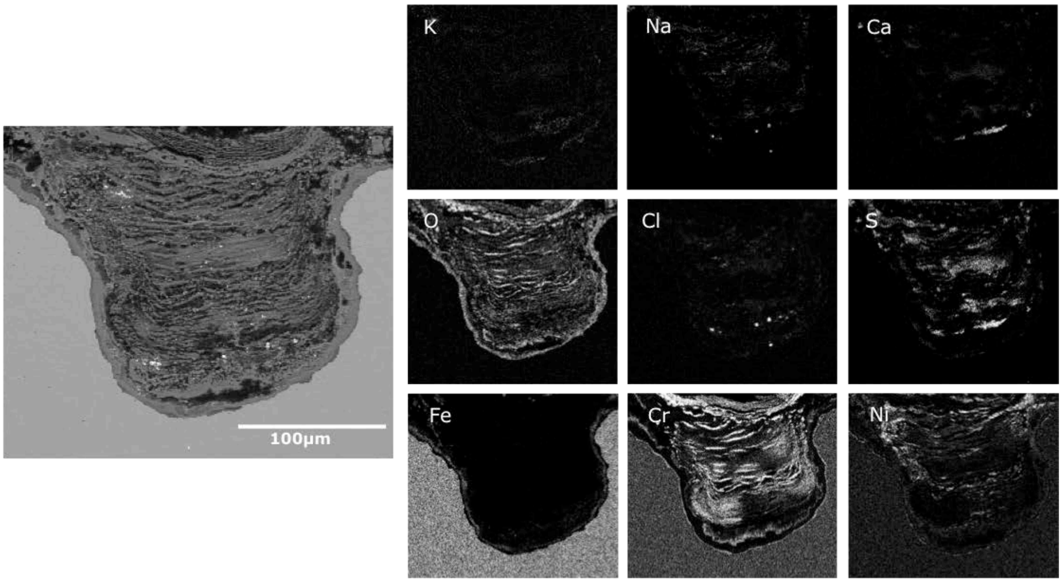


**Figur 28. SEM/EDX analys av ett tvärsnitt av 304L exponerat i 3600 timmar vid 455 °C i position 1.**

***Figure 28. SEM/EDX analysis of a cross section of 304L exposed at 455 °C for 3600 hours at position 1.***

# 5 Analysis of the results

The background for this project is derived from the usually poor estimations on corrosion rate of the superheaters in biomass and waste fired boilers. Hence, this project shares the same background as the KME509 project, performed in the P14 boiler at Händelöverken. By performing this type of extensive exposure matrix in two different boilers, the aim has been to get a more general understanding about how probe exposures can be performed in order to obtain quantitative corrosion rates applicable for estimations of the service life of the installed superheater. Especially the discrepancy between probe and tube exposed samples have been addressed. Better estimations of the superheater corrosion will lead to better plant economy as changing a superheater is usually associated with great costs. Today, the estimated corrosion rate of the superheaters is usually extrapolated from probe measurements, exposed for a certain time (e.g. 1000 hours). Due to the limitations of these estimations, the boiler owners are instead planning upcoming changes of the superheaters by performing thickness measurements of the superheater bundle during the yearly revision.

In addition to increasing the knowledge about quantitative corrosion testing, this project has also performed an extensive matrix of short term deposit testing. By this frequent probe testing and large effort in analysis, the variations in fuel composition have been coupled to the flue gas chemistry and deposit composition, over a period of 6 months. Furthermore, this project has been performed in parallel to a project investigating how the fouling (i.e. deposit build-up) of the boiler is progressing with time. By increasing the knowledge about how the fuel, gas chemistry and deposit composition is connected, the model for fouling may be improved. Hence, this project can be separated in two main parts:

- *Short-term probe exposures*,
  Investigation of how the fuel, flue gas and deposit build up is coupled.

- *Long-term probe and tube exposures*,
  Investigate the kinetics of the corrosion attack by means of probe exposures and if there are any inherent difference between tube and probe exposures.

*Short-term probe exposures*

In this project, 6 successful short term (4 hours) exposures were performed in the period of 6 months. In order to perform these exposures the minimum load of the boiler had to be at least 80%. In each exposure, a cooled probe with 8 samples divided into 2 temperature zones (304 °C and 455 °C) was exposed at the superheater (position 1).

In addition to optical inspection and gravimetry, the deposit material was analyzed with IC, ICP-OES and XRD. From the optical inspection, it was shown that the appearance of the deposit layer was rather constant over time, being uniform and beige. A thicker deposit layer was noticed on the windward side. Even though the exposure time only lasted for 4 hours, the samples had started to corrode. This was especially true for the T22 samples exposed at 455 °C, which experienced some spallation after exposure. Furthermore, by XRD the presence of corrosion products was seen on all exposed samples (e.g. $Fe_2O_3$, spinel type oxide ($Me_3O_4$) and $FeCl_2x2H_2O$). Thus, the deposit probe samples had started to corrode already after 4 hours. This can be due to the effect of being started cold put directly into the hot, corrosive environment. The effect of start-up has also been noticed for the samples exposed in the KME509 project. The deposit composition was throughout all exposures dominated by $CaSO_4$ and alkali chlorides (KCl and NaCl). This was confirmed by ICP-OES and IC analysis, showing a dominance of Ca, Cl and S.

The analysis of the deposit for each exposure was compared with corresponding fuel analysis and flue gas composition with respect to the content of Cl, S and Ca. The results show that the correlation between the fuel, flue gas and deposit composition is rather good. This indicates that the deposits covering the boiler walls do not, to a large extent, interfere with the flue gas, i.e. there is little memory effect in the boiler.

The adherence of the deposit to the ring surface was tested with a method described in section 3.2. Due to the spallation of the T22 samples resulting from poor adhesion of the corrosion product layer, the results of this test were omitted in this analysis. The adherence of the deposit on the 304L samples is good, only about 10% was spallen off in the test. The temperature had an effect on the adherence; the samples exposed at 455 °C showed higher content of lose material than the samples exposed at 304 °C. This could be linked to the higher mass gain obtained by the samples at 455 °C. After the test, the collected deposit material consisted mainly of small deposit particles; no corrosion products were visible in the collected deposit material. The deposit adheres well to the steel surface; the loose deposit material could be attributed to poor adhesion between the particles in the deposit. The presence of corrosion products can result in poor adherence of the deposit to the metal, were corrosion products cause spallation at the corrosion product/steel interface. Since the deposit is still adherent the samples it indicates low corrosion rates.

*Long-term probe and tube exposures.*

This project has successfully exposed corrosion probes up to 3600 hours in a time resolved manner at two positions (before and after) at superheater 2. The probes were mounted in the boiler during revision, at the same time as the test sections of the superheater tube was installed. Hence, both tubes and probes were slowly heated in a mild environment (i.e. oil burning) during the boiler startup sequence after revision. The probes were removed after 24, 1000, 2000 and 3600 hours of exposure. The tubes were removed after 3600 hours of exposure. The probes located after the superheater (i.e. position 2) were removed after 1000 and 3600 hours. The aim of these frequent probe exposures was to obtain information about the corrosion rate over time. The aim of exposing both probes and tubes was to investigate if there is any inherent difference between samples exposed on cooled probes and samples exposed as a part of the superheater loop.

The results show that the corrosion of the probe exposed samples is generally low, in many cases within the margin of error of the method used for measuring the material loss. In fact, the corrosion rate is actually decreasing with time for the samples exposed at position 1. The slow corrosion rate of the long term exposed samples is somewhat contradictory towards the short term exposed samples, where clear evidence of a corrosion attack could be recognized. However, it is worth to again stress that the startup procedure of the short and long term samples were different. The results are also indicating that the gentle startup of the long term samples is actually affecting the long term corrosion behavior. For 304L, the samples exhibited a smooth, protective oxide on the majority of the sample surface. This oxide probably formed during the initial stages of exposure (i.e. during start-up). However, in cases this protective layer has been destroyed. In many cases, a layer of potassium could be seen in connection to the areas with accelerated corrosion attack. This may be remnants of chromate formation, known for destroying the protective properties of stainless steels. However, the results are not conclusive. When the protective layer is destroyed, the diffusion of ions through the scale is fundamentally changed and a local attack is initiated. In addition, this type of corrosion morphology is much more susceptible towards in-diffusion of chloride ions, which will further accelerate the corrosion. The results show that once the protective oxide is destroyed, the 304L steel is not able to heal and the corrosion attack is progressing with time. In those areas where the initial protective oxide is maintained, there are no signs of an accelerated corrosion attack.

In the case of the T22 samples, the corrosion morphology is different compared to the 304L samples. For the low alloy steel, the corrosion attack resulted in a more general degradation, especially at the wind side. However, according to material loss determination, the corrosion rate was low. The T22 material does not contain enough chromium (needs to be at least 11 wt%) in order to form a chromium rich protective oxide. Instead, T22 forms different types of iron oxides (Hematite ($Fe_2O_3$) and Magnetite ($Fe_3O_4$)). These oxides exhibit a much poorer protection against further corrosion and the general degradation seen on the T22 samples agrees well with this type of corrosion attack. However, the initial oxides formed in the mild environment during startup together with a non-corrosive deposit, are expected to some extent decrease the corrosion compared to a sample exposed directly towards the hot, corrosive flue gases.

One important aim of this project was to compare if there exists an inherent arbitrary difference between samples exposed on probes and samples exposed as part of the superheater bundle. Thus, if such a difference exists, corrosion rate measurements by means of probe exposures are by default an inadequate method in estimating the service life of the superheater tubes. The results show that the difference between material losses of probe exposed samples and tube exposed samples is small. In some cases the probes exhibited a slightly higher mass loss, in other the highest mass loss was detected on the tube exposed samples. Thus, the results indicate that there is no inherent difference between tube and probe exposed samples. The differences seen are probably due to other reasons. When performing probe exposures, in which the aim primarily is to estimate the corrosion rate of the superheaters, it is however of great importance that the probes are exposed in such way that they truly mimic the superheaters. This includes for instance that the probes should be started from a cold boiler and during shorter stops the probes should remain inside the boiler (in similarity to the superheater tubes).

# 6 Conclusions

The results from this project combined results from KME 509 show general knowledge of the life time prediction of the superheater materials. This project has successfully executed a comprehensive exposure matrix including 12 probe exposures and 2 test sections in the existing superheater exposed in time resolved manner up to 3600 hours. Of the 12 probe exposures, 6 were of short term character (i.e. 4 hours) investigating the deposit formation. The exposure matrix included 3 materials and 2 material temperatures, performed at two positions in the superheater bundle. The following conclusions have been made within this project; the first three points agree well with the conclusions of the KME 509 project:

- The corrosion rate was generally low of the investigated steels. This correlates well with corrosion rate of the superheaters installed today which show small material wastages (life time today 14 years).
- The startup of the corrosion probes seems to be of great importance for the overall corrosion rate (especially for shorter exposure times). The results indicate that a startup with cold probes directly into a hot boiler affect the corrosion attack negatively.
- The project also investigated if there was any inherent difference between the corrosion rate of probe exposed samples and the superheaters. According to the results, it does not seem to exist such a difference. Hence, probe exposures are a possible way of investigating the potential corrosion rate of superheaters. However, it is important to stress that the probe exposures needs to, as far as possible, mimic the thermal and environmental history of the superheater.
- The short term exposed samples have been used in order to couple the fuel composition, flue gas chemistry and deposit formation. Special focus has been attributed to the sulphur and chlorine levels. In general, there is good agreement between the different Cl/S ratios of the fuel, flue gas and deposit for the different exposures.

# 7 Goal fulfilment

The overall goal of this project has been to generate new knowledge in order to facilitate the development of models for determine the service life of superheaters and thus, improve the plant economy. By the comparably large exposure matrix with both probe and tube samples, resolved in time, valuable information about the progress of the corrosion rate has been obtained. The project does also aim for increasing the understanding of deposit build-up and fouling.

The project has also been evaluating the possibility to increase the steam temperature by at least 50 °C for waste fractions. According to the results, the corrosion rate was not increased dramatically for the higher temperature (455 °C compared to 304 °C). However, at the higher temperature, locally high corrosion rates can be observed on the 304L sample.

The project also investigated if there was any inherent difference between the corrosion rate of probe exposed samples and the superheaters. According to the results, it does not seem to exist such a difference. Hence, probe exposures are a possible way of investigating the potential corrosion rate of superheaters. However, it is recommended that efforts are made that the probes are installed and started in such way that they mimic, as far as possible, the situation of the superheater. This includes for instance start-up from cold boiler and more than one exposure time. Furthermore, the exposure time of the probes should preferably be longer than 1000 hours.

The project showed how the deposit composition varied over a 6 month period and connected the composition in the deposit to the fuel analyses and flue gas chemistry. The deposit composition for the 6 different tests was similar and a correlation to both fuel analyses and flue gas chemistry was made.

This project has shared the same overall goals as the parallel KME509 project. By combining the results from these two projects, the overall conclusion is that the results, from a lifetime assessment point of view, are similar. This includes for instance the effect of the startup sequence of the probes and that there does not seem to exist any inherent difference between probe and tube exposures.

# 8 Suggestions for future research work

This project has enlightened various aspects that are of importance when performing probe exposures for quantitative estimations of the service life of the superheater tubes. However, the results obtained within the project have also raised some suggestions for further studies. One important aspect to investigate more thoroughly is the effect of the start-up procedure on the corrosion attack. As it seems, the corrosion attack is more severe when the probe is started directly into a hot waste fired boiler compared to a sample heated up in a mild environment before being exposed towards the corrosive atmosphere characterized by a waste fired boiler. If the goal is to obtain corrosion rates for quantitative estimations of the service life of the superheater tubes, this needs to be addressed.

# 9 Literature references


1. A Stålenheim, P.H., *Korrosion i avfallsförbränningsanläggningar*, 2004.
2. Andersson, S., et al., *Sulfur recirculation for increased electricity production in Waste-to-Energy plants.* Waste Management, 2014. **34**(1): p. 67-78.
3. Andersson S, B.E., Bäfver L, Claesson F, Davidsson K, Froitzheim J, Karlsson M, Pettersson J, Steenari B-M,, *Minskad pannkorrosion med svavelrecirkulation*, 2010.
4. Brostrom, M., et al., *Sulfation of corrosive alkali chlorides by ammonium sulfate in a biomass fired CFB boiler.* Fuel Processing Technology, 2007. **88**(11-12): p. 1171-1177.
5. Folkeson, N., Pettersson, J., Pettersson, C., Johansson, L-G., Skog, E., Svensson, J-E., *Fireside corrosion of stainless and low alloyed steels in a waste-fired CFB boiler; The effect of adding sulphur to the fuel* Materials Science Forum, 2008. **595-598**: p. 289-297.
6. Henderson, P., Szakalos, P., Pettersson, R., Andersson, C., Hogberg, J., *Reducing superheater corrosion in wood-fired boilers.* Materials and Corrosion-Werkstoffe Und Korrosion, 2006. **57**(2): p. 128-134.
7. Henderson, P.J., et al., *Corrosion testing of superheater steels for 600 degrees C steam in biomass/co-fired boilers*. Advanced Heat Resistant Steels for Power Generation, ed. R. Viswanathan and J. Nutting1999. 507-516.
8. Michelsen, H.P., Frandsen, F., Dam-Johansen, K. and Larsen, O. H., *Deposition and high temperature corrosion in a 10 MW straw fired boiler.* Fuel Processing Technology, 1998. **54**(1-3): p. 95-108.
9. Montgomery, M. and A. Karlsson, *In-situ corrosion investigation at Masnedo CHP plant - a straw fired power plant.* Materials and Corrosion, 1999. **50**(10): p. 579-584.
10. Montgomery, M., A. Karlsson, and O.H. Larsen, *Field test corrosion experiments in Denmark with biomass fuels. Part 1: straw-firing.* Materials and Corrosion, 2002. **53**(2): p. 121-131.
11. Montgomery, M. and O.H. Larsen, *Field test corrosion experiments in Denmark with biomass fuels. Part 2: Co-firing of straw and coal.* Materials and Corrosion, 2002. **53**(3): p. 185-194.
12. Salmenoja, K., *Field and Laboratory Studies on Chlorine-induced Superheater Corrosion in Boilers Fired with Biofuels*, in *Faculty of Chemical Engineering*2000, Åbo Akademi: Åbo. p. 102.
13. Skog, E., Hansson, H., Hansson, S., Svensson, J.-E., Johansson, L. -G, Pettersson, C., Pettersson, J., Jonsson, T., Halvarsson, M., Folkeson, N., Asteman, H., Hagström, M., Pettersson, J. B. C., Davidsson, K., Brink, K.-E., Tuiremo, J., Aspelin, T., Wilson, A., Heikne, B., Arnesson, B., Eriksson, K., and Gerdin, P., *KME-132 Material evaluation and research in the waste fired boiler at Händelö*, 2004. p. 163.
14. Skog, E., Folkeson, N., Pettersson, C., Pettersson, J., Svensson, J.-E., Andersson, B-.Å., Enestam, S., Toivonen, T., Tuiremo, J., Wilson, A.,

Arnesson, B., Heikne, B. and Jonasson, A., *KME309 Material evaluation and research in the waste fired boiler P14 at Händelö Part II*, 2005.
15. Skog, E., Lindqvist, O., Folkeson, N., Johansson, L. -G, Pettersson, J., Pettersson, C., Svensson, J.-E., Ljungström, E. and Steenari, B.-M., *Inverkan av svaveltillsatser på överhettarkorrosion, emissioner och askkvalitet i en bioeldad anläggning*, W.i.S. STEM, Editor 2006.
16. Viklund, P., et al., *Corrosion of superheater materials in a waste-to-energy plant.* Fuel Processing Technology, 2013. **105**: p. 106-112.
17. Viklund, P., et al., *Effect of sulphur containing additive on initial corrosion of superheater tubes in waste fired boiler.* Corrosion Engineering Science and Technology, 2009. **44**(3): p. 234-240.
18. Jesper Pettersson, J.-E.S., Erik Skog, Lars-Gunnar Johansson, Nicklas Folkeson, Jan Froitzheim, Sofia Karlsson, Erik Larsson, Nicklas Israelsson, Sonja Enestam, Johanna Tuiremo, Anna Jonasson, Bertil Arnesson, Bengt-Åke Andersson, Bengt Heikne, *KME411 - Evaluation of different fuel additives´ ability to master corrosion and deposition on steam superheaters in a waste fired CFB-boiler*, 2010.
19. Davidsson, K., Gustafsson, G, Herstad Svärd, S., Jones, F., Niklasson, F., Ryde, D., *WR38 - Askans betydelse för rötslams goda samförbränningsegenskaper*, W. Refinery, Editor 2012.

# 10 Publications

This project has not yet led to any publications.

# Appendices

## Appendix A
"Operating data and fouling factors in project KME-514" by WSP.

## Appendix B
"Returbränsle P6, KME projektet" by Fortum.